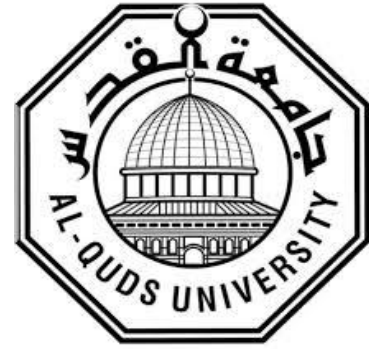


Deanship of Graduate Studies

Al-Quds University



**Synthesis and Characterization of Polyacrylamide co
acrylic acid Carbon Nanotube Nanocomposite for
Pharmaceutical Packaging Applications**

Taghreed Akrm Muhammad Taqatqa

M.Sc. Thesis

Jerusalem, Palestine

2022 – م 1443هـ

**Synthesis and Characterization of Polyacrylamide co
acrylic acid Carbon Nanotube Nanocomposite for
Pharmaceutical Packaging Applications**

Prepared by: Taghreed Akrm Muhammad Taqatqa

Faculty of Higher Education

Department of Chemistry

Al-Quds University

Supervisor: Dr. Sami Makharza – Hebron University

Co-Supervisor: Dr. Wadie Sultan

This thesis submitted in partial fulfillment of requirement
for the degree of Master of Applied and Industrial
Technology, Al-Quds University

2022 / 1443ھ

Al-Quds University

Deanship of Graduate Studies

Applied and Industrial Technology



Thesis Approval





**Synthesis and Characterization of Polyacrylamide co acrylic acid
Carbon Nanotube Nanocomposite for Pharmaceutical Packaging
Applications**

**Prepared by: Taghreed Akrm Taqatqa
Registration Number: 21712716**

**Supervisor: Dr. Sami Makharza
Co-Supervisor: Dr. Wadie Sultan**

Master thesis submitted and accepted, Date: 28\5\2022

The names and signatures of the examining committee are as follow

- 1. Head of Committee: Dr. Sami Makharza** **Signature:** 
- 2. Co-supervisor: Dr. Wadie Sultan** **Signature:** 
- 3. Internal Examiner: Dr. Mahmod Alkhatib** **Signature:** 
- 4. External Examiner: Dr. Derar Smadi** **Signature:** 

Jerusalem/ Palestine

2022/1443

Dedication

At the end of my research, I would like to dedicate it firstly to my beloved land "Palestine". As well as to Al-Quds University; the University of Creativity and Excellence my first incubator at the Bachelor's level.

Also, I dedicate it to my supervisor Dr. Sami Makharza , and co-supervisor Dr. Wadie Sultan who provided me continuous support whenever I was in need. I will never forget to dedicate this achievement to Mrs. Maryam Faroun; the researcher at Nano lab who did not hesitate a moment to help me.

To my beloved husband, Hussein, who, whatever I said, I will not be able to thank him, my husband, who was my first supporter to go in this way and did not hesitate for a moment for giving me financial and moral support.

Mom, Dad, and all my family gave me bigger support and always encouraged me to complete my education.

My two little girls, Mayar and Hazzar, are bearing my absence. One day they grow up and be proud of their mother and forgive me for shortcomings towards them.

My second family, my husband's family and particularly my husband's mother who supported me in various ways.

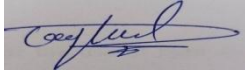
.All my friends and people in my life who love me and remember me

I dedicate my research..

Declaration

I certify that this thesis submitted for the degree of master, is the result of my own research, except where otherwise acknowledged, and this thesis has not been submitted for the higher degree to any other university or institution.

Taghreed Akrm Taqatqa.

Signed: 

Date:28/5/2022

ACKNOWLEDGEMENT

First of all, we thank Allah for everything. Then we would like to express our sincere appreciation and heartfelt gratitude to our supervisor, Dr.Sami Makharza, and Dr. Wadie Sultan for their creative guidance, intellectual support, encouragement, and patience throughout the course of this work. We are grateful for their excellent hospitality and wonderful attitude, and we feel very fortunate to have had this opportunity to study under his supervision. We also like to express our gratitude to Dr. Ibrahim Afaneh for his continued support of us.

We are deeply indebted to our friends for their steadfastly stood up to me like a true friend, and willing to lend a hand in times of need. We are most grateful and enormously indebted to our families for their love, support and encouragement during this period. They provided a lot of inspiration and zeal for us to work hard.

Also, we would like to thank Al-Quds University for the use of their facilities and supply of materials and for their kindness dedication to our success. Finally, we are thankful for Hebron University and BeitJala Pharmaceutical Company because they helped us in the project.

Taghreed Taqatqa

Abstract

The MWNT functionalized COOH is prepared by the carboxylation on the surface of the MWNTs. The MWNT-COOH was used to be incorporated in poly acrylamide-co-acrylic acid (Poly(AAm-co-AA)) to study the thermal, mechanical properties, as well as the swelling test. Different concentrations of Poly(AAm-co-AA) (5, 2.5, 1.25, and 0.9%) with different concentrations of CNTs-COOH (0.03 and 0.015 %) were used to prepare Poly(AAm-co-AA) /CNTs-COOH nanocomposite by simple casting method. Thermal properties were studied by using Differential Scanning Calorimetric (DSC), the results show that the thermal properties were enhanced by the incorporation of CNTs into the Poly(AAm-co-AA) matrix. The glass transition temperature (T_g) was increased from 55 of neat Poly(AAm-co-AA) to 70°C at 0.03, 0.015% CNTs-COOH. The crystallinity was increased to a certain extent. This indicates that part of the polymer shifted from the amorphous form to the crystalline form, which leads to a reduction in the distances between the polymer chains, and this is evidence of an increase in its hardness. The young's modulus was increased to 400% at 5% Poly(AAm-co-AA) and 0.03% CNTs-COOH. The swelling of Poly(AAm-co-AA) with different concentrations increased by adding CNT-COOH nanoparticles due to an increase in hydrogen bonding from -COOH. The FT-IR spectra of Poly(AAm-co-AA)/CNTs nanocomposite confirm the strong bonding between polymer and nanoparticles in different functional groups. Briefly, the incorporation of CNT into Poly(AAm-co-AA) polymer matrix improves the thermal, and mechanical properties of polymer due to strong hydrogen interaction between polymer and CNTs particles.

Contents		Page
1.	Chapter one: Introduction	1
	1.1 Polyacrylamide-coacrylic acid	1
	1.2 Carbon Nanotubes CNT's	2
	1.3 Properties of Carbon Nanotubes Nanocomposites	5
	1.3.1 Electrical properties of CNTs	5
	1.3.2 Mechanical properties of CNTs	5
	1.3.3 Thermal properties of CNTs	6
	1.4 Polymers/CNT's Nanocomposites	6
	1.5 Nanomaterial in Pharmaceutical Science and Pharmaceutical Technology	8
	1.6 Nanomaterials in Pharmaceutical Packaging	11
	1.7 polymers / CNT's Nanocomposites in Pharmaceutical technology	12
	1.8 Objective	13
2.	Chapter Two: Literature Review	14
	2.1 Introduction	14
	2.2 Superior properties of carbon nanotubes	14
	2.2.1 Thermal Properties of polymer/ CNT's Nanocomposite	14
	2.2.2 Mechanical Properties of Polymer/ CNT's Nanocomposite	14
	2.2.3 Swelling ratio of Polymer/ CNT's Nanocomposite	17
	2.3 Quality Assurance (FT-IR of polymer with carbon nanotubes)	19
3.	Chapter Three: Materials and Methods	21
	3.1 Materials and Equipment	21
	3.2 Methods	22
	3.2.1 Preparation of Poly(AAm-co-AAc) Thin Films	22
	3.2.2 Preparation of Poly(AAm-co-AAc) /CNT-COOH Films	23
	3.3 Measurement	27
	3.3.1 Thickness	27
	3.3.2 Thermal Properties	27
	3.3.3 Mechanical Properties	28
	3.3.4 Fourier-Transformed Infrared Spectrometer (FT-IR)	28
	3.3.5 Swelling Test	28
4.	Chapter four : Result and Discussion	29
	4.1 Introduction	29
	4.2 Superior Properties of Poly(AAm-co-AAc), Poly(AAm-co-AAc)/ CNTs	29
	4.2.1 Thermal Properties	29
	4.2.2 Mechanical Properties	33
	4.2.3 Swelling	35
	4.2.4 FT-IR	37

	4.2.5	Thickness	40
5.	Conclusions		42
6.	References		43
	المُلخَص بالعربية		47

Listof Tables		Page
NO.	Title	
Table1.1	Electrical properties of CNTs	5
Table1.2	Mechanical properties of CNTs	6
Table1.3	Thermal properties of CNTs	6
Table 2.1	Superior Properties of CNTs	15
Table 3.1	Matrix of P(AAm-co-AA)/CNT's nanocomposite preparation.	25
Table 4.1	DSC results	32
Table 4.2.a	Swelling ratio results of P(AAm-co-AA)	36
Table 4.2.b	Swelling ratio results of P(AA-co-AA)/CNT-COOH	36
Table 4.3	FT-IR results for each of P(AAm-co-AA) film,CNT-COOH,P(AAm-co-AA)/CNT-COOH nanocomposite	40
Table 4.4	Thickness results for polymer alone by calculation and caliber and P(AAm-co-AA)/CNT-COOH by caliber	41

ListofFigures		Page
No.	Title	
Figure 1.1	Possible mechanism for obtaining of poly(acrylamide- co -acrylic acid) in presence of “initial radicals” formed from initiator	1
Figure 1.2	polyacrylamide- co acrylic acid	1
Figure 1.3	(a) single-walled carbon nanotube, (b) multi-walled carbon nanotube	3
Figure 1.4	nanomaterial application	4
Figure1.5	Stress-Strain curve Carbon	4
Figure 1.6	Nanomaterial in pharmaceutical applications	9
Figure1.7	CNT in pharmaceutical applications	11

Figure 1.8	Nanomaterials in Pharmaceutical Packaging	12
Figure3.1	photograph of equipment used. A) FT-IR, B) DSC, C) Mechanical Tester	21
Figure 3.2	Samples of Poly(AAm-co-AA)Films.	23
Figure 3.3	Preparation of (PAAm-co-AAc) /CNT Nanocomposite Films	24
Figure 3.4	Poly(AAm-co-AA)/MWNT-COOH nanocomposite films	25
Figure 4.1	Thermal properties of Poly(AAm-co-AA).(DSC)	30
Figure4.2.a	Thermal properties of Poly(AAm-co-AA)/CNT-COOH (5.0mg/ml:0.3mg/ml). (DSC)	31
Figure4.2.b	Thermal properties of Poly(AAm-co-AA)/CNT(5.0mg/ml:0.15mg/ml). (DSC)	31
Figure4.2.c	Thermal properties of Poly(AAm-co-AA)/CNT(2.5mg/ml:0.3mg/ml).(DSC).	32
Figure4.3.a	Stress-Strain of P(AAm-co-AA)	34
Figure4.3.b	Stress-Strain of P(AAm-co-AA)/CNT(5.0:0.015)mg/ml	34
Figure4.3.c	<i>Stress-Strain of P(AAm-co-AA)/CNT(5.0:0.3)mg/m</i>	35
Figure4.4.a	FTIR Spectra of P(AAm-co-AA).	37
Figure4.4.b	FTIR Spectra of Functionalized CNT-COOH	38
Figure4.5.a	FT-IR spectra of P(AAm-o-AA)/CNT(5.0:0.3)mg/ml	39
Figure4.5.b	FT-IR spectra of P(AAm-o-AA)/CNT(2.5:0.3)mg/ml	39

LIST OF ABBREVIATIONS	
AAC	Acrylic acid
APS	Ammonium persulfate
ATR-FTIR	Attenuated Total Reflection - Fourier-Transferred Infrared Spectrometer
CNT	Carbon nanotube
CVD	Chemical vapor deposition
DSC	Differential Scanning Calorimetry
DDSs	Smart drug delivery systems
DFU	Diabetic foot ulcers
EB	Elongation at break
EDC	N-(3-Dimethylaminopropyl)-N'-ethylcarbodiimide hydrochloride
FTIR	Fourier-Transferred Infrared Spectrometer
GX	Glucuronoxylan
HDPE	High-density polyethylene
IR	Infrared
MMWNT	Magnetic Multi-walled nanotube
MWNT	Multi-walled nanotube
NHS	N- Hydroxysuccinimide
NTs	Nanoparticles
PHBV	Poly(3-hydroxybutyrate-co 3-hydroxy valerate)
PLA	Poly (lactic acid)
Poly(AAm-co-AA)	Poly (acryl-amide-co-acrylic acid)
Poly(AAm-co-IA)	poly(acrylamide-co-itaconic acid)
Poly(AM-co-SMA)	Poly(acrylamide-co-sodium methacrylate)
PP	Polypropylene
PS	Polystyrene
PVA	Poly(vinyl alcohol)
PVDF	Poly vinylidene fluoride
SEM	Scanning electron microscope
SPEs	Screen-printed electrodes
SPR	Surface Plasmon resonance
SR	Swelling ratio
SWNT	Single-walled nanotube
TEM	Transmission electron microscopy
TEMED	N,N,N',N'-tetramethylethylenediamine

TG	Glass transition temperature
TM	Tensile modulus
Tm	Melting temperature
WRC	The water retention capacity

Chapter One: Introduction

1.1 Poly acryl amide- co- acrylic acid

Poly acrylamides are one of the most extensively used water-soluble polymers and should be referred to as poly (acryl-amide-co-acrylic acid). They are made by partial hydrolysis or copolymerization with acrylic acid, with APS as the initiator, TEMED as the activator, and BIS as the cross-linking agent. As shown in Figure 1.1

The electrostatic connection in poly (AAm-co-AAc) is strong, resulting in a more stable co-polymer[1].

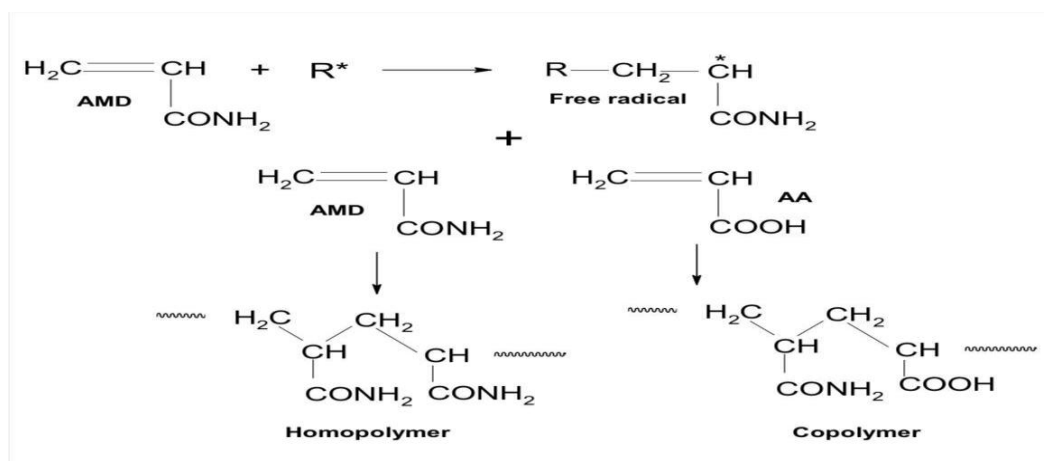


Fig.1.1 Possible mechanism for obtaining poly(acrylamide- co -acrylic acid) in presence of “initial radicals” formed from initiator[2].

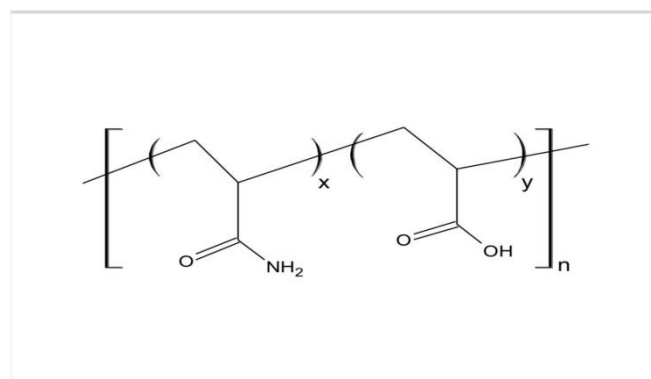


Fig.1.2 Chemical structure of Polyacrylamide- co acrylic acid

The hydrogels show unusual swelling patterns, indicating that they are extremely sensitive to pH. The swelling of polymeric networks is influenced by the polymer's composition, such as acrylic acid concentration, and the nature of the swelling media,

such as pH: swelling rate rose as pH and acrylic acid content in the hydrogel increased. The swelling of the hydrogels abruptly changes when the swelling media is changed from distilled water to a high pH solution, demonstrating the polymers' intelligent character[1].

The single TG in the DSC analysis revealed that the two polymers in the hydrogel have strong miscibility; this behavior was due to the polymers' ability to create H-bonding, which has been reported for polymers with similar properties[1].

Superabsorbent polymer hydrogels, for example, Poly(Acryl amid-co-Acrylic acid), are a special type of swellable polymeric substance. SPHs may absorb disproportionately huge amounts of different activation fluids and swell dependent on their unique chemical crosslinks, which include both hydrogen and ionic bonds, thanks to their three-dimensional crosslinked polymeric network structure. Their hydrophilic functional groups are responsible for their superabsorbent properties, which results in the development of an insoluble gel rather than dissolution. SPHs have increasingly been used in a wide range of applications in recent decades as a result of their versatility and suitability, as summarized below[3].

Because of their high hydrophilicity, low toxicity, and biocompatibility, hydrogel materials have attracted a lot of attention. Hydrogel application suitability is determined by various parameters, including swelling performance, equilibrium swollen ratio, and mechanical strength from a dry to a highly swollen condition, according to studies. The hydrogel's swellability is determined by its response mechanism to external stimuli like pH and temperature. Hydrogels have been discovered as having a slow temperature response rate and low mechanical strength. Hydrogels have been modified using a variety of ways to improve their applicability for diverse applications, including crosslinking with nanoparticles[3]. This is what we shall do in our research to improve the polymer's qualities.

1.2 Carbon Nanotubes CNT's

Carbon nanotubes, which are large-scale allotropes of carbon with a cyclic nanostructure with a diameter of approximately 1 nm and a length of about 100 nm, were discovered using transmission electron microscopy (TEM) in 1991[4], kicking

off the discipline of carbon nanoscience. Single-walled (SWNTs) CNTs are made up of a single graphene layer rolled into a perfect cylinder with a typical diameter of 1–1.5 nm, while multi-walled (MWNTs) CNTs are made up of multiple concentric cylindrical graphene layers with typical diameters ranging from 5 nm to hundreds of nanometers [5],[6]. As shown in Figure 1.3. The carbon arc-discharge method (using arc-vaporization of two carbon rods), the chemical vapor deposition (CVD) method (using hydrocarbon sources: CO, methane, ethylene, acetylene), and the laser-ablation method (using graphite) are all common methods for manufacturing high-quality carbon nanotubes [7].

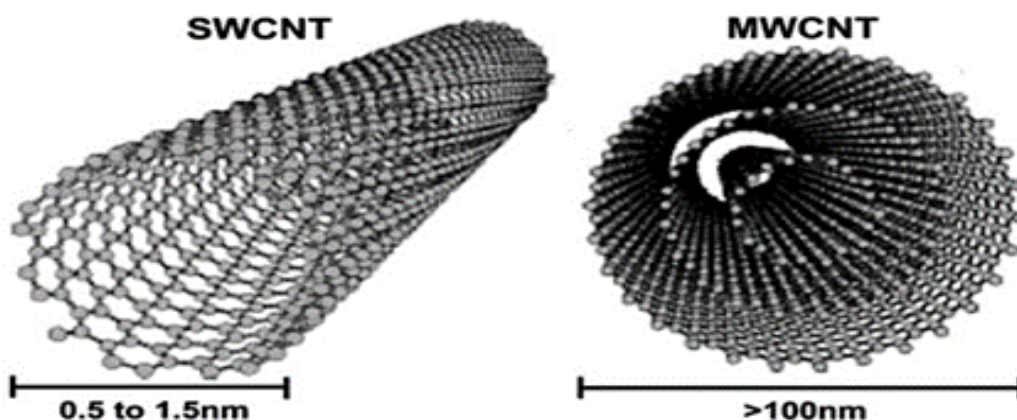


Fig.1.3(a) single-walled carbon nanotube, (b) multi-walled carbon nanotube

Carbon nanotubes have gained a lot of attention because of their unique structure, which includes the arrangement of carbon atoms in their shells, mechanical strength, electrical capabilities, and chemical stability, which allows them to conjugate or adsorb with a variety of medicinal compounds [3].

CNTs have revolutionized a variety of scientific sectors due to their properties. Medicine and pharmacy, for example, are combined to create functional materials for biosensor diagnosis and biomedical scaffolding[3]. Also in many applications, as shown in Figure 1.4 for example , energy, biology, electronics, tools, and agriculture. CNTs, on the other hand, have a substantial disadvantage over other carbon nanostructures in that they typically contain metallic nanoparticles that remain electrochemically active and pose a hazardous threat. It can be avoided by eliminating metallic contaminants and performing pretreatment. [6].

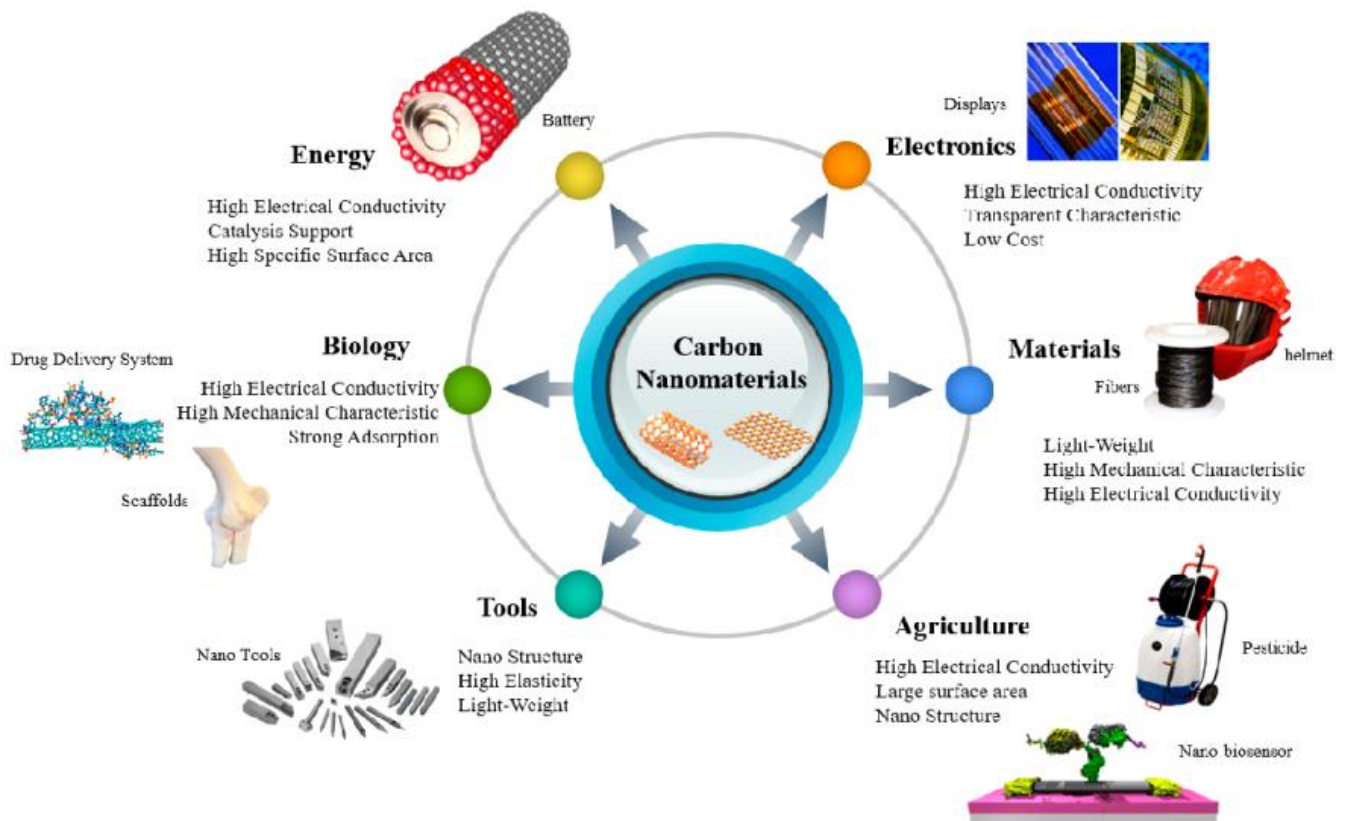


Fig 1.4 Applications of Nanomaterials in different fields[8].

Carboxylation of MWNTs:

A sulfuric acid/nitric acid combination solution and MWNTs were used to carboxylate the surface of the nanotubes. After the final product was dried, a carboxyl-functionalized MWNTs-COOH sample was obtained. [9]. Figure 1.5 which is depicted the carboxylation process of MWNTs. The MWNT-COOH we are used in our research.

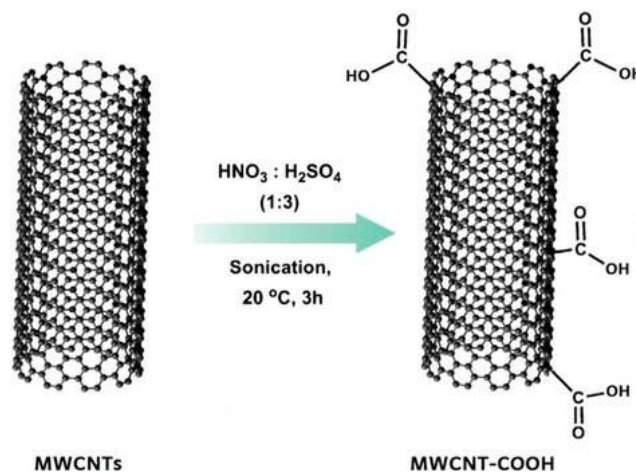


Fig 1.5 Chemical structure of Functionalized MWCNT-COOH[10].

1.3 Properties of Carbon Nanotubes Nanocomposites

1.3.1 Electrical properties of CNTs

Table (1.1) shows the electrical properties of CNTs in chiral forms, as well as their high stiffness and axial strength as a result of C-C (sp²) bonding. As a result, each unit retains the fourth valence electron, which is delocalized over all atoms and contributes to the electrical character of CNTs. Depending on the type of chirality, CNTs can be conducting or semi-conducting [11], [12]. P-type semiconductors are used to make semiconducting SWNTs. Because MWNTs are made up of numerous tubes of SWNTs, they are unlikely to be a 1D conductor[6].

Table 1.1 Electrical properties of CNTs

Electrical properties	Electrical conductivity	Resistivity	References
SWNTs	(10 ⁴ s / cm)	(0.34*10 ⁻⁴ – 1.0*10 ⁻⁴) ohm.cm	[6] [13]
MWNTs	Non-conductors	Non-conductors	[11]

1.3.2 Mechanical properties of CNTs

Vander Waal's forces can deform two nearby CNTs, according to the first TEM report of radial elasticity [14]. When a load is applied to a composite structure, the radial direction elasticity of CNTs is critical for the development of CNT nanocomposites and their mechanical properties, in which embedded tubes are subjected to substantial deformation in the occasional direction. CNTs have ideal potential since the C-C bonds found in graphite are among the strongest. They are also the stiffest and hardest structures. CNTs have been demonstrated to be elastic and do not break when bent in TEM studies [15], [16]. Table (1.2) showed the mechanical properties of single and multi-walled carbon nanotubes and the differences between them.

Table 1.2 Mechanical properties of CNTs

Mechanical properties	Young's modulus	Tensile strength	Elongation%	References
SWNTs	320-1470 GPa	13-52 GPa	>50% Improved the elastic range	[14],[5]
MWNTs	1-1.2 TPa	20-90 GPa	Improvement the elongation%	[17],[18]

1.3.3 Thermal properties of CNTs

The thermal conductivity and low-temperature specific heat in CNTs reveal direct proof of the phonon band structure's 1-D quantization [19]. Despite their modest size, quantum effects are significant.

The addition of pristine and functionalized NTs to various materials can double thermal conductivity for loadings of only 1%, indicating that NT composite materials may be useful for several factors that influence thermal properties, such as the number of phonon-active modes, the length of the phonons' free path, and boundary surface scattering [20]. The atomic arrangement, diameter, and length of the tubes, the number of structural flaws and morphology, and the presence of contaminants in the CNTs all influence these attributes [21]. And as shown in Table 1.3, which indicates that single-walled have higher conductivity than multi-walled due to these attributes.

Table 1.3: Thermal properties of CNTs.

CNTs	Thermal conductivity	References
SWNTs	3,000 W/K	[22]
MWNTs	200 W/m K	[22]

1.4 Polymers/CNT's Nanocomposites

Polymeric biomaterials were first used in the 1940s[6]. There has been a huge change in the usage of polymers in biomedical applications.

There are two types of polymers used as biomaterials in biomedical applications: Polysaccharides such as starch, cellulose, and carbohydrate polymers are examples of natural-based polymers[6].

Natural polymers offer the advantage of biological recognition, which aids cell adherence and function, but they have drawbacks such as weak mechanical qualities[6]. Many of them are also in short supply, resulting in higher prices. Poly (lactic acid) (PLA), and poly vinyl alcohol (PVA), are examples of B-synthetic polymers. The elastic modulus, deterioration rate, tensile strength, and microstructure are all repeatable mechanical and physical qualities of synthetic polymers, their surfaces, on the other hand, are largely hydrophobic and devoid of cell recognition signals[6].

Carbon nanostructures, such as carbon nanotubes (CNTs), have sparked business and academic attention because they improve the mechanical, chemical, and biological features of natural and synthetic polymers' cellular adhesion tendency in bio applications [3]. Despite the fact that various polymers have been employed in biomedical applications, no single biopolymer can cover all of the needs for drug delivery systems and biomedical scaffolds. As a result, biopolymers are frequently mixed with materials in order to achieve optimal performance and specific biological responses. Because of their unique mechanical, chemical, biological, and physical features, carbon-based nanostructures have recently gained a lot of attention as biomaterials. Because they combine the benefits of polymers with carbon, carbon-based nanocomposites are the most promising materials for bioapplications such as drug delivery and tissue engineering. (biocompatibility and biodegradability) and those of carbon nanostructures [23],[24].

In comparison to conventional systems, carbon-based nanocomposites have particular characteristics that make them appropriate biological materials for bone formation and therapeutic carrier agents. They have excellent mechanical properties due to their compact structure or stiffness, and their small size facilitates entry into cellular compartments. They are also the best choice because of their ease of surface chemistry modification and large capacity in terms of loading therapeutic and imaging molecules [25]. And another recent study for CNT has shown MWCNT modified by

dendrimer has been used for the delivery of the drug doxorubicin which is used in breast cancer treatment [26].

Self-healing nanocrystalline polymeric hydrogels have the potential to be highly useful in the treatment of microcracks. They can be used to protect the environment, cure wounds, provide thermal insulation, and regulate medicine flow into the body. [27]. Bone tissue is also a current trend in polymeric nanocomposites. It regenerates bone tissue at the defect site since it is absorbable and biodegradable.

This review includes some of the most often used analytical techniques, such as spectroscopy and electron microscopy.

The mechanical force that has a significant impact on tissue outgrowth, reproduction, and cell attachment, as well as the physical features of biomaterials, have been discussed, such as particle size, pore size. [28].

These studies and the compatibility between CNTs and polymers in terms of properties support the idea of the study that we did.

1.5 Nanomaterial in Pharmaceutical Science and Pharmaceutical technology

As shown in Figure 1.6, Pharmaceutical nanotechnology offers new tools, scope, and prospects for illness detection and therapy, all of which are likely to have a substantial impact. Pharmaceutical nanotechnology has emerged as a discipline with enormous potential as a carrier for Spatio-temporal delivery of bioactivity and diagnostics and as a source of smart materials for tissue engineering, as well as a specialized field for drug delivery, disease treatment, and diagnosis using nanoengineering tools[29].

Cancer, cardiovascular disease, and infection control are the key areas where Nanomedical products have had an impact. Nanoparticles for pharmaceutical applications are in line with a new technology that aims to improve drug delivery system solutions. The rate of absorption, metabolism, distribution and excretion of the drug or related substances in the body must all be influenced positively by drug delivery methods. They must also allow the medication to bind to its target receptors and influence their signaling and activity, as well as be capable of being hydrolyzed

into fragments and excreted through normal excretory channels after usage. Daunoxome®, Doxil®, and Ambisome® are only a few nanotechnology-based products and delivery systems that are now on the market. This technique has the potential to aid in the identification, diagnosis, treatment, and prevention of disease [29].

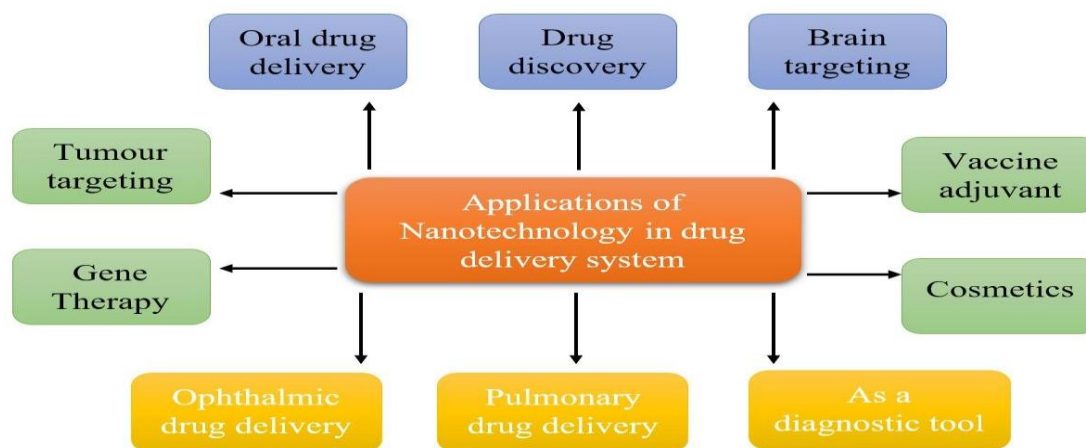


Fig 1.6 Nanomaterial in pharmaceutical applications[30].

In recent years, cellulose nanoparticles (CNs) have been successfully used in scientific disciplines as one of these new uses. The CNs demonstrate significant potency in fine-tuning the microstructures and kinetics of Nano-levels abundant sustainable materials[31].

The advantages of CNs over other nanoparticles are numerous: they are human and environmentally friendly, recyclable, and have a large amplitude, making them readily available and unreliable. Furthermore, a large number of (-OH) groups on the surface make CNs adaptable and customizable, which is significant for pharmaceutical processing. CNs have applications in a range of fields[31].

Another study looked into the use of polysaccharide-forming hydrogel materials in the design of Ag nanoparticles of various shapes and sizes.

The hydrogels where they are used as covering agents for the fabrication of Ag nanoparticles are polysaccharide-based hydrogels. One potential polysaccharide to form a hydrogel is glucuronoxylan (GX), which has been used as a vector for the targeted release of various drugs of the pH response to switching on and off [32].

Wound healing dressings contain GX-Ag nanoparticles. The amount of collagen in

the wound and the tensile strength of the epithelial tissue determines the wound's method of action[32].

Diabetes is one of the world's most serious health concerns, with around 25% of diabetic people at risk of developing foot complications (diabetic foot ulcers, DFU), and wound healing is poor. Nanoparticles have shown extraordinary effects in the wound healing process because of rapid breakthroughs in Nanomedicine. When α -Fe₂O₃ nanoparticles are utilized, DFU responds well, and the wound healing process is accelerated. When there is inflammation, neutrophils and macrophages penetrate the wound and increase their number within 1-3 hours of the wound, resulting in the development of superoxide radical anions, which slows down the healing process. Because CeO nanoparticles are biocompatible, they were used in the DFU treatment. [33].

Nanoparticles are a promising cancer research candidate. Because they are directly connected with sickness in the target and have a controlled release behavior, nanoscale-based smart drug delivery systems (DDSs) have blazed the way in the pharmaceutical field. Because of their small size and inexpensive manufacturing costs[34].

Screen-printed electrodes (SPEs) are utilized as immunosensors in conjunction with nanoparticle smart devices, and nanoparticle-modified SPEs are used to diagnose disorders including Parkinson's and Alzheimer's. Because Ag nanoparticles have surface Plasmon resonance (SPR) properties, they were used for ultrasensitive analysis. The SPR property is increased further by covering the nanoparticles with graphene. Magnetic nanoparticles are coated with lanthanides to generate a bright complex for bimodal imaging[34].

Also, In Figure 1.7 shows the CNTs as tablets, microcapsules, nanocapsules, etc. This prompted us to continue working on our studies.

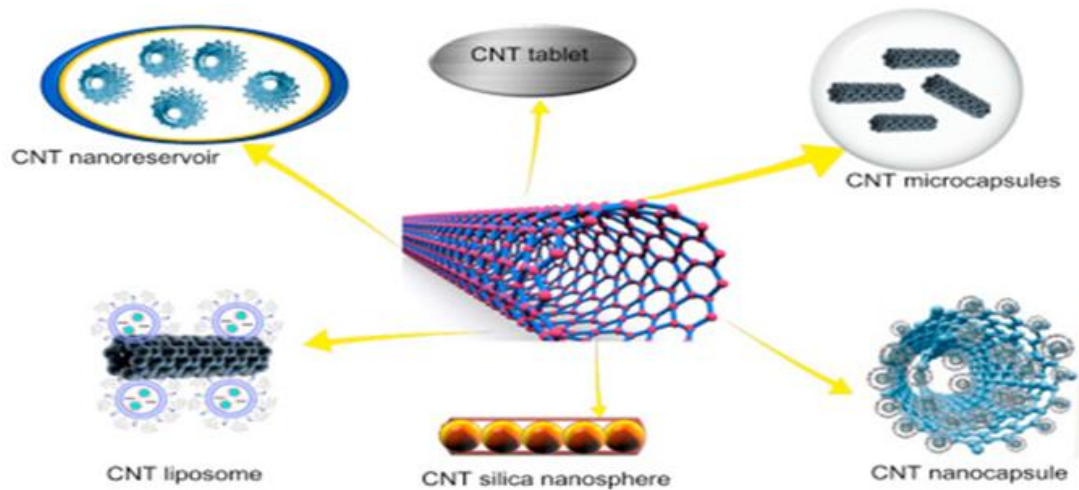


Fig1.7 CNT in pharmaceutical applications[35]

1.6 Nanomaterials in Pharmaceutical Packaging

The main goal of packaging materials with a single layer or multilayer films, whether polymers, metal foils, and coatings, is to maintain the quality and components of the product. It is important to consider the effects of appropriate packaging design in reducing waste for environmental sustainability, especially where waste and shelf-life are linked. The polymeric structure of the packing determines the diffusion of gases and liquids through the polymeric sheets. Higher crystalline leads in lesser free volume, and the orientations of the molecular chains result in a better barrier by producing a more twisting diffusion channel. The most crucial consideration is to have a thorough grasp of the kinetic process in order to ensure that the chosen substance is both efficient and non-toxic. It's worth noting that various properties of nanoparticles can be altered throughout the manufacturing process to assure quality and quality control in accordance with norms and laws [36]. Figure 1.8, showed the many applications of Nanoparticles (Nano-sensors) in pharmaceutical packaging.

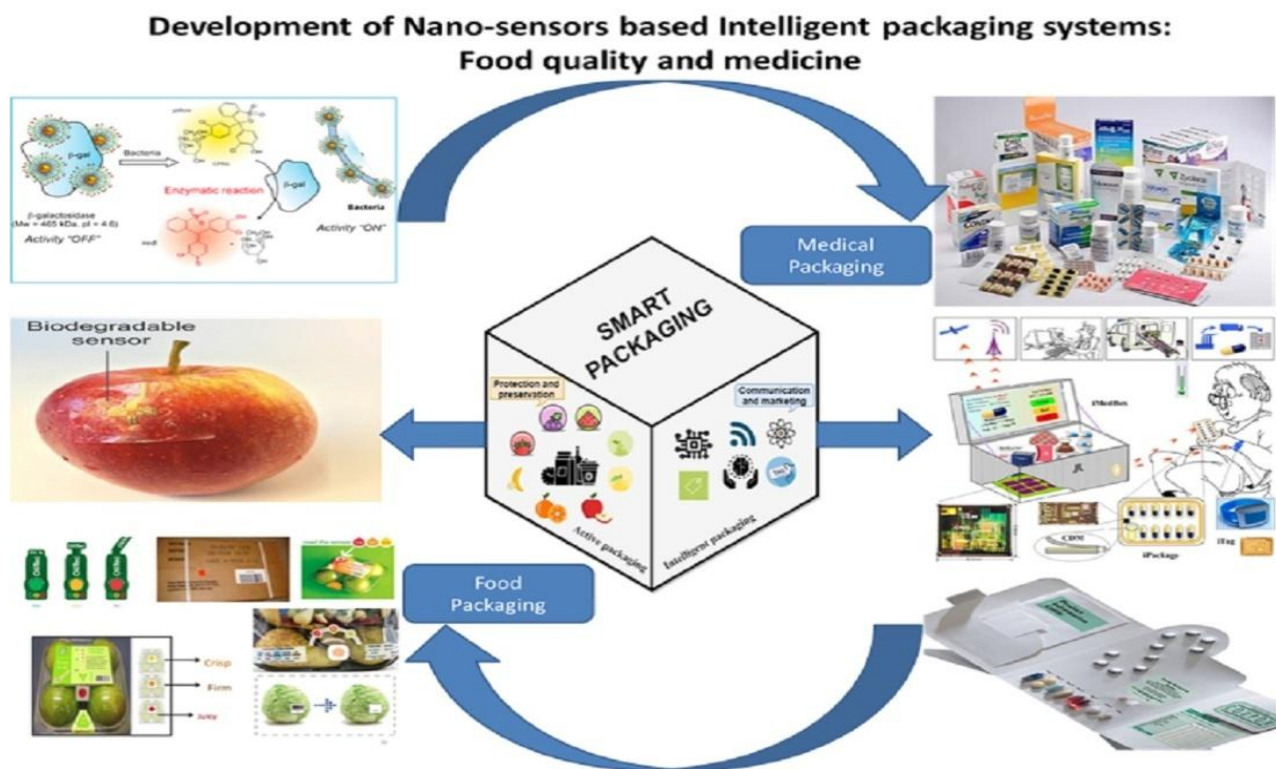


Fig 1.8 Nanomaterials in Pharmaceutical Packaging.[37]

1.7 polymers / CNT's Nanocomposites in Pharmaceutical technology

Carbon-based nanostructures, such as carbon nanotubes (CNTs), have piqued the interest of both industry and academia because they increase the mechanical, chemical, and biological properties of natural and synthetic polymers in bioapplications[3]. Despite the fact that various polymers have been employed in biomedical applications, no single biopolymer can meet all of the requirements for drug delivery systems and biomedical scaffolds[38]. In comparison to traditional systems, CNTs have significant characteristics that make them appropriate biological materials for the production of treatment carrier agents. Because of their compact structure or stiffness, they have excellent mechanical properties; their small size facilitates entry into cellular compartments, and their ease of surface chemistry modification and large capacity in terms of loading therapeutic and imaging molecules have made them the best choice[38].

Natural biopolymers and artificial polymers have been used in therapeutic applications in recent studies, and to meet all of the biomedical scaffolds drug delivery and best performance, this study was done by combining polymers with CNT compounds. They have been used for tissue engineering and drug delivery due to their small sizes, large surface area, and ability to interact with cells/tissues, as it improves the mechanical, chemical, and biological properties of Cellular adhesion[3].Hydrogels can aid in the repair of tiny fractures. They can be utilized to protect the environment, cure wounds, provide thermal insulation, and regulate medicine flow into the body[27]. Bone tissue is also a current trend in polymeric nanocomposites.

1.8Objectives

In general, a great deal of research has gone into improving packing materials using various approaches. Packaging is a sort of enhanced material used to extend the shelf life of pharmaceutical items and make communication between them and consumers easier.

The goal of this study is to look at how nanoparticles are used in pharmaceutical packaging.

These nanoparticles give the polymer extraordinary characteristics, allowing it to move toward active packaging.

As a result, the Poly (AAm co-AAM)/MWCNT-COOH hydrogel nanocomposite films will be synthesized, and the mechanical, thermal, and swelling properties of the polymer with MWCNT-COOH Nanocomposites will be compared to hydrogels without MWNT-COOH. In the field of pharmaceutical packaging, these nanocomposites are crucial.

Chapter two : Literature Review

2.1 Introduction

Pharmaceutical packaging is important for keeping pharmaceutical products clean, healthy, safe, and increasing the shelf life, whether food or pharmaceutical materials. There are a lot of efforts to develop these packages by using nanoparticles to improve properties of polymers as mechanical and thermal properties. It can also be used as a barrier on packaging materials to reduce permeability and extend the shelf life.

In this chapter, we will review the thermal, mechanical, swelling properties of CNT's/polymer nanocomposite differential scanning calorimetry (DSC) and Fourier transform infrared spectroscopy (FTIR).

2.2 Superior Properties of CNT's

2.2.1 Thermal Properties of polymer/CNT's Nanocomposite

Researchers are interested in the crystallization and melting properties of polymers and MWCNT nanocomposites because crystal structures and polymer crystals play a vital impact in influencing mechanical capabilities. The breakdown temperature of polymers/MWCNT is greater than that of polymers, indicating that the addition of MWNTs improves the thermal stability of nanocomposites, suggesting that the nanocomposites had increased thermal stability and resistance to thermal deterioration. As shown in Table (2.1) as the addition of 1.5W% MWNT to the polymer PHBV led to thermal stability.[38], as well in Polypropylene /0.3% MWNT.[39].

2.2.2 Mechanical Properties of Polymer/ CNT's Nanocomposite

The mechanical properties of polymers and MWCNT nanocomposite were examined, including tensile strength (TS), elongation at break (EB), and tensile modulus (TM).

The presence of MWCNTs in the matrix inhibited the mobility of the blends' molecular chains, resulting in an increase in the TS of composites.

Because MWCNTs are robust, homogeneously dispersed MWCNTs can provide stiffness and hardness to polymers via interfacial contact. As a result of this study, MWCNTs induced a considerable increase in all mechanical characteristics of

polymers (TS, TM, and EB). As shown in Table 2.1 like PVA, PS, and PHBV, which is an unusual phenomenon.

Table 2.1 Superior Properties of CNT's

Polymer	CNTs	Test	Result	Method	Reference
PVA	1% MWNT	The stiffness	Low at RT 150MPa	TEM	[40]
		Elastic modulus	Increase 1.8		
		The Young's modulus	1.6		
PS	1% MWNT	The elastic	Increase 36%	TEM	[40]
		stiffness	42%		
		Neat polymer modulus	1.2GPa		
		Tensile strength	Increase 25%		
PHBV	1.5W% MWNT	Mechanical tensile modulus and Strength	Improved 48% 49%	Raman spectroscopy (morphology and structure of MWCNT) Transmission electron microscopy (TEM) Differential scanning calorimetry (DSC) Thermogravimetric analysis	[38]
		Thermal behavior	Thermal stability		
		mechanical resistance	increases mechanical resistance (48%) To provide a good dispersion Not significantly Slightly improve (after MWCNT)		

			37%	(TGA)	
PP	0.3% WMWT	The tensile strength	Increased 18.4%	By melt processing methods by	[39]
		Flexural strength	5.2%	employing extruder and injection molding techniques	
		Modulus of elasticity	45%		
		The impact strength	Decreased 18%		
		Elongation at break	(690)%		
		Thermal behavior	Thermal analysis data revealed that the MWCNT addition slightly increased the crystallization peak onset and peak maximum temperatures of PP under non-isothermal conditions		
Polyurethane	2% WMWNT	Thermal behavior	Thermal stability	SEM TEM Dynamic mechanical analysis (DMA) thermal analysis (DTA)	[41]
		Modulus	Increased >10C		
		tensile strength	increased		

HDPE	2% W MWNT	Thermal properties	high decomposition temperature (resistance to thermal degradation) and thermal stability	Thermogravimetric analyses (TGA) SEM Rockwell Hardness	[42]
		Mechanical properties	enhanced hardness, 65.22% 54.69%	Taber abrasion weight loss (mg) Impact strength (KJ/m ²)	
			22.4% increased the young's modulus		

2.2.3 Swelling ratio of Polymer/ CNT's Nanocomposite

In research Bardajee, et al., optimized the elements impacting the hydrogel's water swelling (monomer concentration, ammonium persulfate concentration, and N-N'-methylene bis acrylamide concentration) and examined the effect of various environmental circumstances (pHs, time, and temperature). The rate parameters for swelling of the hydrogel without MMWNT are stated to be around 28minutes, indicating that the hydrogel's swelling ability is reduced when compared to MMWNT/Hydrogel. Because of the nanocomposite's great sensitivity to pH, it can be classified as a smart material with applications in pharmaceuticals due to its repeated swelling–deswelling behavior in pH = 2 and PH = 9. Because of the nanocomposite's response to tetracycline hydrochloride release at various pHs, this MMWNT / Hydrogel was shown to be acceptable for drug release at pH = 7.4. The VSM results revealed that the MMWNT/ hydrogel has a superparamagnetic characteristic, which decreases drug release when an external magnetic field is present[43].

In addition, a study by Mohammadnezhad, et al., where poly (acrylamide-co-itaconic acid)/MWCNTs were created. The results showed that increasing the MWCNT

content improved the hydrogel's stability, which can be attributed to the MWCNTs' hydrophobic nature as well as the increased cross-linker density. The MWCNT concentration, swelling time, pH, temperature, and salt content all influenced the swelling behaviors of Poly (AAM-co-IA) and Poly (AAM-co IA)/MWCNTs. When the swelled polymer and polymer/MWCNTs were heated, the water retention value for Poly(AAM-co-IA) dropped to zero after 7 hours, whereas Poly(AAM-co-IA)/MWCNTs retained 13% of the absorbed water. In the presence of the MWCNT, the P(AAM-co-IA)'s retention capacity (WRC) increased (10 wt %). The adsorption of Pb (II) from an aqueous solution was investigated using a hydrogel nanocomposite. The Poly (AAM-co-IA)/MWCNTs demonstrated better adsorption behavior toward Pb(II) than the polymer hydrogel. This aids in the removal of Pb(II), which is one of the most dangerous contaminants in water, even at low quantities, and can harm the kidneys, central nervous system, and liver. Pb (II) levels in drinking water and wastewater are allowed to be 0.05 mg/L and 0.005 mg/L, respectively. [44]

Because solvent absorption into the space between the polymeric chain network causes the Nano gels to expand, the swelling behavior of hydrogels is critical. Drug distribution throughout the hydrogels may be influenced by the swelling proportion of hydrogel composites, which is proportional to the hydrogel mesh size, altering the proliferation and differentiation of encapsulated cells. [45]

The researchers Liu, Z., Z. Yang, and Y. Luo, in this study, looked at the swelling ratios of MWCNTs-COOH reinforced poly (acrylamide co sodium methacrylate) hydrogels. They looked at the swelling ratios of MWNTs-COOH reinforced poly (acrylamide co sodium methacrylate) hydrogels. As the MWNTs-COOH loading is lowered from 2.5 wt percent to 1.5 wt percent to 0.75 wt percent at 25°C, the ESR of hydrogels steadily increases. According to the experimental results, the Poly(AM-co-SMA)/MWNTs-COOH nanocomposite hydrogel with 0.75 wt% MWNTs-COOH has a higher ESR value and a larger pore size. The MWNTs-COOH increase the pH sensitivity and reversibility when the nanocomposite hydrogels are buffered with buffer solutions of various pH values. When nanocomposite hydrogels are switched from an alkaline to an acidic buffer solution, they react swiftly and in a short period of time. As a result of the development of extra hydrogen bonds. In acidic solutions, the

swelling ratio (SR) decreases, while in alkaline solutions, it increases. PH =1.4, PH=13 at 25°C [43].

2.3 Quality Assurance (FT-IR of polymers with CNTs)

ATR-FTIR analysis of the samples[46], in the investigation confirmed the establishment of a covalent link between the functionalized surface of the PVDF/MWCNT membrane and the laccase. Due to the existence of COOH-MWCNTs, the significant peak detected at 1400 cm^{-1} for all three samples can be attributed to -OH bonds in carboxylic acid functional groups. The peak at 1671 cm^{-1} for the membrane sample immersed in EDC/NHS solution is broken into two new peaks at 1568 and 1659 cm^{-1} , which are identical to peptide C=O stretch and N-H bend, respectively, which are related to the amide groups. [46].

The FTIR spectra of Polymer-MWCNT, MWCNT-COOH, and MWCNT-OH samples [39], revealed intense bands at 3436 cm^{-1} . Asymmetric methyl stretching bands at 2960 cm^{-1} and asymmetric/symmetric methylene stretching bands at 2923 , 2853 cm^{-1} are detected in the Polymer-MWCNT and MWCNT-COOH spectrum. These groups are commonly thought to be positioned at the defect spots on the sidewall surface. The spectrum bands at 2923 and 2853 cm^{-1} for MWCNT-OH diminish dramatically, implying that the alkyl chains have been cleaved from the nanotubes' surface. On the MWCNT-COOH surface, the C-O bands indicative of carboxyl functional groups can be seen at 1732 , 1708 , and 1560 cm^{-1} . The carboxylate anion stretch mode is linked to the peak at 1560 cm^{-1} . The Polymer-MWCNT and MWCNT-OH spectra [39] do not show these bands.[39]

In another study by Kim, et al., the peak positions symmetrical to C=O stretching, $\nu(\text{C=O})$, are assigned to values in the range of $1650\text{--}1750\text{ cm}^{-1}$ in the (Kim et al., 2018) study, showing small peak shifts of the -COOH derivatives. The spectrum of the PAA film showed a peak at $\nu(\text{C=O})$ of 1693 cm^{-1} , while raw CNTFs showed a peak at $\nu(\text{C=C})$ of 1573 cm^{-1} and a peak identical to CH₂ stretching vibrations at 2910 cm^{-1} . When compared to the PAA film, the C=O peak in the CLCNTF-(PVA/PAA) spectrum was observed at a higher frequency of 1720 cm^{-1} , indicating that ester bonding was formed between the -COOH groups of PAA and the -OH groups of PVA after thermal condensation [47].

In research by Salem, et al., [48], the IR absorption bands of the MWCNT/gelatin–PVA nanocomposite remained the same, despite relative increases in the strength of the peaks at 1630 and 1547 cm^{-1} . The rise in the intensity of these bands is attributable to MWCNT C=C stretching in conjunction with Amide-I C=O stretching and N–H bending for amide II and I, according to the research. [48].

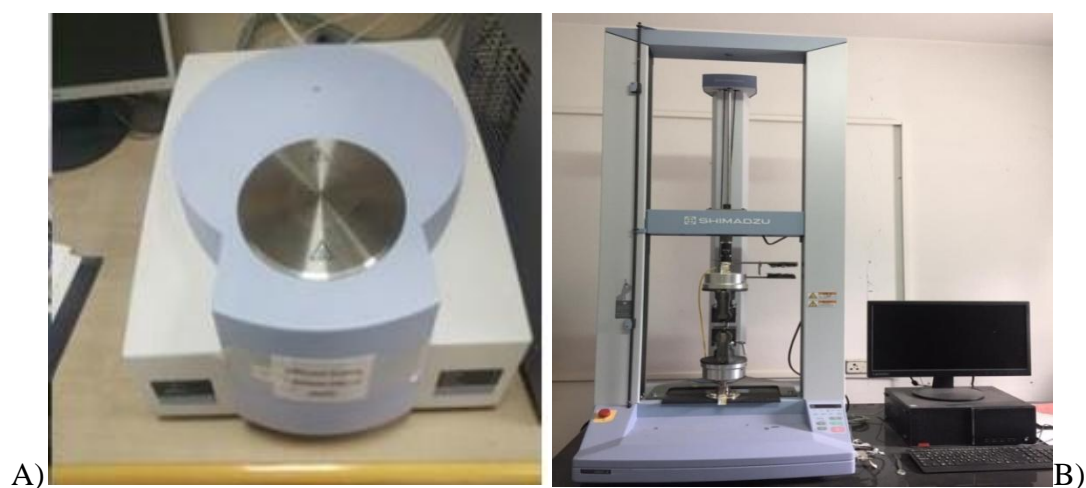
3. Chapter Three: Materials and Methods

3.1 Materials and Equipment:

The Polyacrylamide co acrylic acid powder, 80+%, M.wt = 150000-520000g/mol and $D=0.75\text{g/ml}$. Carbon nanotube, multi-walled, carboxylic acid functionalized, extent of labeling >8% carboxylic acid diam. $\times L9.5*1.5\mu\text{m}$ are purchased from Sigma Aldrich.

The following equipment was used at Nano lab: Spin coater with timer reaches to 30sec and speed reaches to 1000rpm, model 37600 Mixer, Analytical Balance, Digital Caliper (STAINLESS HARDENED) 0-150mm.

DSC analysis was performed using DSC Perkin Elmer 4000 (heated for 450 0C) with a heating rate of 10 C/min and under nitrogen atmosphere Figure3.1 A, Mechanical Test Machine Figure3.1 B. The Fourier transform infrared (FTIR) spectrometer of Bruker IFS 66/S, that equipped with liquid nitrogen- cooled MCT detector and aKBr beam splitter Figure3.1 C, this equipment refers to physics lab at Al-Quds university.





C)

Fig 3.1: photographs of A) DSC, B) Mechanical Tester, C) FT-IR

3.2 Methods

3.2.1 Preparation of Poly (AAM-co-AAc) Thin Films

A 5, 2.5, 1.25, 0.9 wt. % of Poly(AAm-co-AA) solutions were prepared under continuous stirring for 30 min at room temperature. Afterwards, the Poly(AAm-co-AA) solutions were casted on Petri dishes and then spin coated at different speed (200- 550 rpm) with different times (5, 15, 30, 60s). In addition to opaque appearance that produced from 5% Poly(AAm-co-AA). As a result, samples using casting method were prepared and allowed to dry in an incubator at room temperature for 3 days to be ready for characterization.



Fig 3.2. Samples of Poly(AAm-co-AA) Films

3.2.2 Preparation of (PAAm-co-AAc) /CNT Nanocomposite Films

Different concentration of MWNT-CNT was prepared using dilution factor from a stock solution of CNT(0.3mg/ml). The diluted solution was divided into 5 parts to add AAm-co-AA and prepare Poly(AAm-co-AA)/CNT nanocomposite solutions with 5, 2.5, 1.25,0.9wt% Poly(AAm-co-AA). These four concentrations of Poly(AAm-co-AA)/CNT nanocomposite were sonicated using bath sonication at RT for 30 min and ultrasonicated for two minutes to obtain a homogeneous solution.

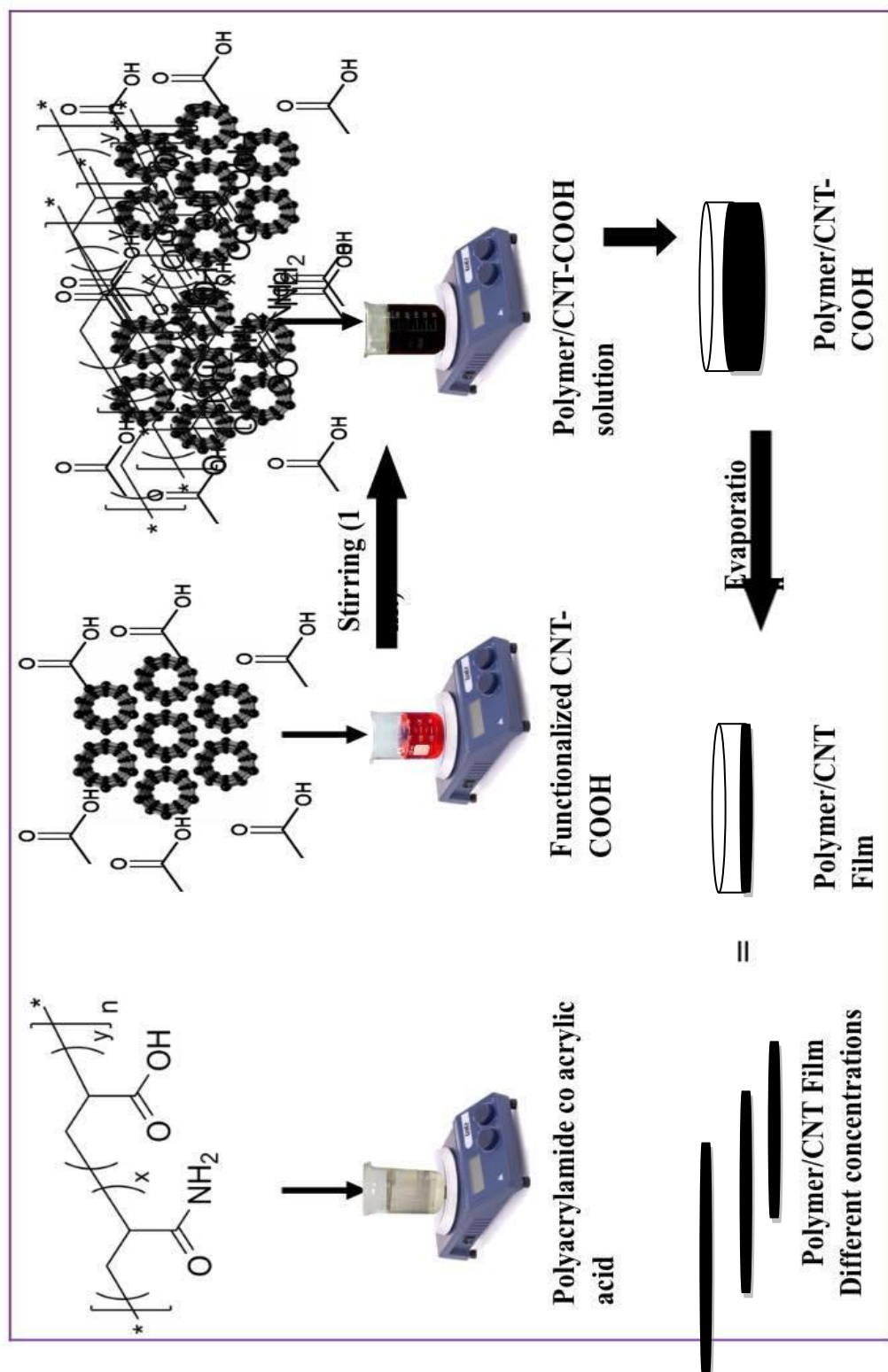


Fig 3.3: Preparation of Poly (AAm-co-AAc) /MWNT-COOH Nanocomposite Films

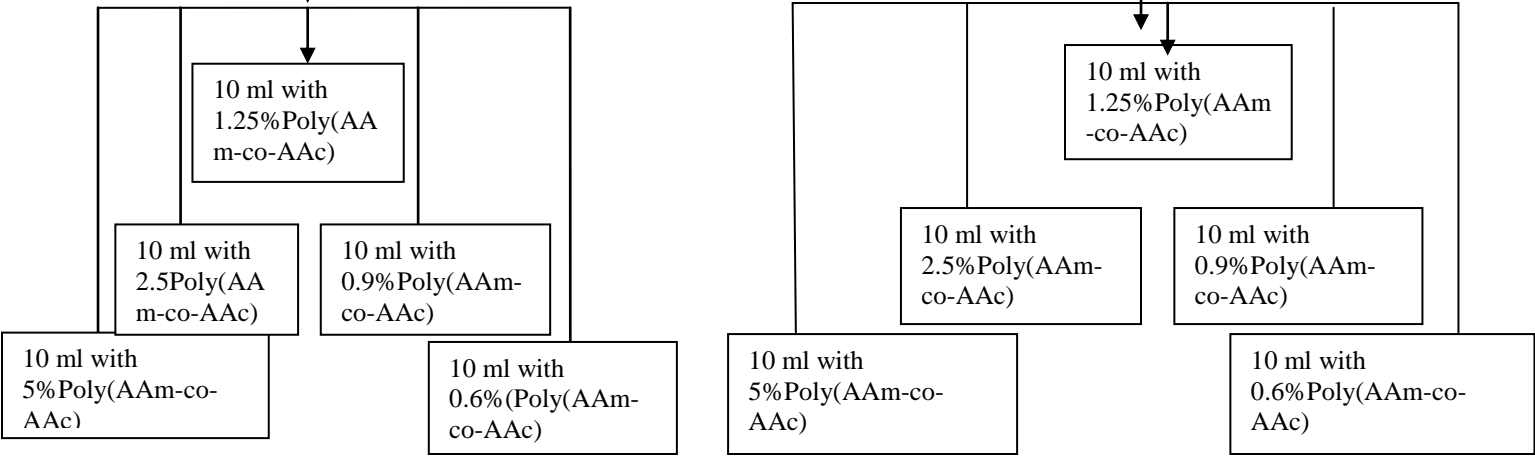
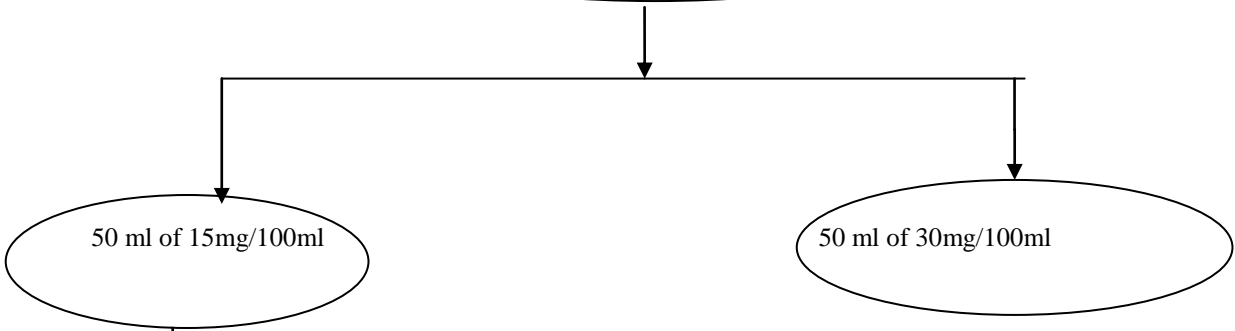


Fig 3.4: Poly(AAm-co-AA)/MWNT-COOH nanocomposite film

Table 3.1 :Matrix of Poly(AAm-co-AA)/MWNT-COOH nanocomposite preparation

No.	Code	Conc.of MWNT-COOH %		Conc.of Poly(AAm-co-AA) %				
		0.03	0.015	5	2.5	1.25	0.9	0.6
<u>1</u>	P ₅ C _{0.03}	<u>X</u>		<u>X</u>				
<u>2</u>	P _{2.5} C _{0.03}	<u>X</u>			<u>X</u>			
<u>3</u>	P _{1.25} C _{0.03}	<u>X</u>				<u>X</u>		
<u>4</u>	P _{0.9} C _{0.03}	<u>X</u>					<u>X</u>	
<u>5</u>	P _{0.6} C _{0.03}	<u>X</u>						<u>X</u>
<u>6</u>	P ₅ C _{0.015}		<u>X</u>	<u>X</u>				
<u>7</u>	P _{2.5} C _{0.015}		<u>X</u>		<u>X</u>			
<u>8</u>	P _{1.25} C _{0.015}					<u>X</u>		
<u>9</u>	P _{0.9} C _{0.015}						<u>X</u>	
<u>10</u>	P _{0.6} C _{0.015}							<u>X</u>

MWNT-COOH Nanocomposites



Bath sonication at RT for 30min

Pouring of different volume

Drying at room temperature for 3Days

Characterization

3.3 Measurement:

3.3.1 Thickness

The thickness of Poly(AAm-co-AAc) thin films was measured using a digital caliper and calculations that depend on weighing the sample that was cut into squares, then measuring the volume according to the equation: Volume = mass/ density.

The volume calculation is used for thickness calculation according to the following equation:

Volume of cube = length* width* height (thickness).

The thickness of Poly(AAm-co-AAc) / CNT films were determined by using the digital caliper, the thickness of each sample was measured at 4 different locations. The thickness of Poly(AAm-co-AAc) and Poly(AAm-co-AAc) / MWNT-COOH nanocomposite were measured as described with Poly(AAm-co-AAc) samples.

3.3.2 Thermal Properties

DSC was performed for 5%, 2.5%, 1.25%, 0.9%, 0.6% of polymer films and for samples contained different concentrations of MWNT-COOH with different concentrations of Poly(AAm-co-AAc).

A 3.0 mg of each sample was cut using a scissors and weighed on a digital balance, the samples were sealed inside DSC pans, the changes in its heat capacity are tracked as changes in heat flow. This process provides thermal information as glass transition temperature, melting/crystallization behavior, degree of crystalline, solid-solid transitions, polymorphism, cross-linking reactions, specific heat, purity determination, and decomposition behavior.

The heating program was performed in the range from 25 °C to 200 °C and then cooled to 25 °C at a rate of 10 °C to obtain melting and crystallization temperature. The sample was reheated to 400 °C at the same rate to obtain glass transition temperature and degradation temperature.

3.3.3 Mechanical Properties

The tensile properties (TS) and elastic modulus for all films were performed using Universal Mechanical Test Machine. Mechanical properties of material provide information about the mechanical resistance and its suitability for our application.

The films were cut into rectangular strips (2×4 cm) with a thickness maintained at (0.01_0.05) mm. The basic idea of a tensile test is placing a sample between two clamps, which pull the material until it breaks. The force and the elongation are measured and the plot of stress versus strain can be generated.

A mechanical test was performed only for high concentrations of Poly(AAm-co-AAc), (5%).

The 2.5%, 1.25%, 0.9% PVA are not applicable in this machine.

3.3.4 Fourier-Transferred Infrared Spectrometer (FT-IR)

The FTIR is a technique used as a fingerprint of the sample depends on IR radiation that passes through the sample, some of the IR radiation absorbed and some of it transmitted. The resulting spectrum represents the molecular absorption and transmission.

FT-IR can supply a qualitative analysis about each kind of samples and determine the functional groups decorated the polymer matrix and loaded CNTs.

The absorption spectra in the IR region (4000-400 cm⁻¹) were taken and discussed.

3.3.5 Swelling Test

The swelling were calculated by immersing the weighted samples in the phosphate buffer pH=7.2 for 20 minutes, Thereafter, the film was removed, dried, and weighted in order to measure the amount of adsorbed solution by the film sample. The samples were dried at a temperature of 400⁰C in an oven and then weighing them again to calculate swelling using the following equation: **Swelling ratio= ((M2-M1)/M1)*100%**

M1: Initial weight of film. **M2:** After immersing in the phosphate buffer over night

Chapter Four: Results and Discussion

4.1 Introduction

In this chapter the results were divided into thermal properties of multi-walled carbon nanotube with Poly(AAm-co-AA), mechanical properties of MWNT-COOH with Poly(AAm-co-AA), swelling films, and solubility of MWNT-COOH with the polymer. All samples were characterized via FTIR, DSC and mechanical testing machine.

4.2 Superior Properties of Poly(AAm-co-AA), Poly(AAm-co-AA) MWNT-COOH

4.2.1 Thermal Properties of Poly(AAm-co-AA) with MWNT-COOH

The thermal properties of Polymer/MWNT-COOH were investigated by using a differential scanning calorimeter. The glass transition temperature of 2.5% Poly(AAm-co-AA) is 55°C. As shown in Figure (4.1). After the addition of MWNT-COOH to the polymer, it was increased to reach the value of 70°C at a 0.03%, 0.015% concentrations of MWNT-COOH with 5% polymer, and 65°C of 2.5% Poly(AAm-co-AA) / 0.03% MWNT-COOH. As shown in Figures (4.2.a, b, and c). Respectively, this behavior is attributed to the strong bonding between MWNT-COOH and the polymer matrixes. That means a very good enhancement in thermal properties for the nanocomposite compared with the neat polymer. The melting temperature for the Poly(AAm-co-AA) is around 290°C. By the addition of 0.03% MWNT-COOH for both polymer concentrations 2.5% and 5%, the melting temperature is 250 °C and 2.5% Poly(AAm-co-AA) / 0.03% MWNT-COOH the $T_m=247^\circ\text{C}$. The difference in the T_m among both concentrations of the polymer is due to the spaces or the volume between the polymer chains being reduced in the lower polymer concentration.

In comparison to the free polymer, the depth of the T_m peak was increased in all nanocomposites thermograms based on the % of crystallinity. This suggests that a portion of the amorphous section becomes crystalline, implying that the presence of CNTs improves closed packing. The above findings are consistent with those found in a search for nanocomposite containing PLA-g-AA copolymer and MWNT-OH [49]. T_g of the hybrid composites is linked to a cooperative motion of long-chain segments,

which could be hampered by the MWNT-OH. As a result, PLA-g-AA/MWNT-OH observed higher T_g than the copolymer, as expected.

It's possible that the higher T_g of PLA-g-AA/MWNT-OH hybrids is due to the MWNT-OH phase's ability to make chemical interactions with hydroxyl group sites offered by PLA-g-carboxylic AA's acid groups. Excess MWNT-OH could have separated the inorganic and organic phases and reduced their compatibility, resulting in an increase in the (T_g) value. In addition, as the MWNT-OH level increased up to 1 wt%, the T_m decreased. The significant decrease in T_m of PLA-g-AA/MWNT-OH is due to the MWNT-OH impeding polymer chain movement, making polymer organization more difficult, as well as the hydrophilic feature of MWNT-OH producing poor adhesion with hydrophobic PLA. [49]

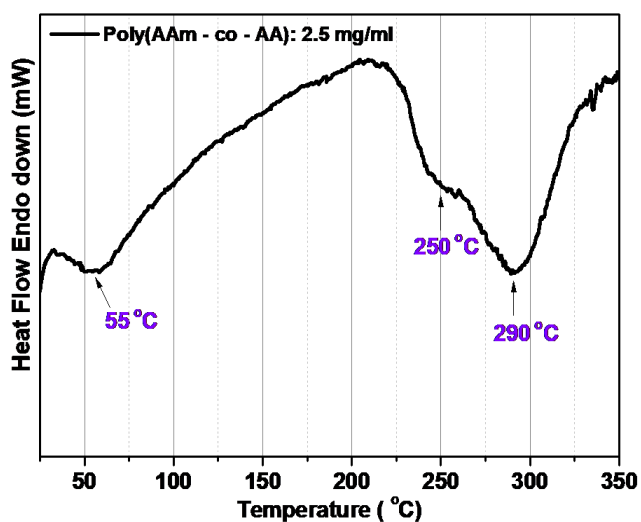


Fig 4.1: DSC thermogram of Poly(AAm-co-AAc)

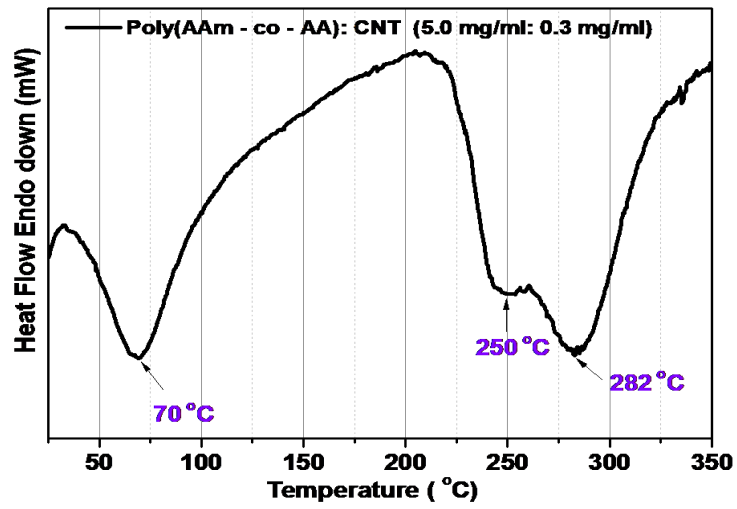


Fig4.2.a :DSC thermogram of Poly(AAm-co-AA)/CNT-COOH (5.0mg/ml:0.3mg/ml)

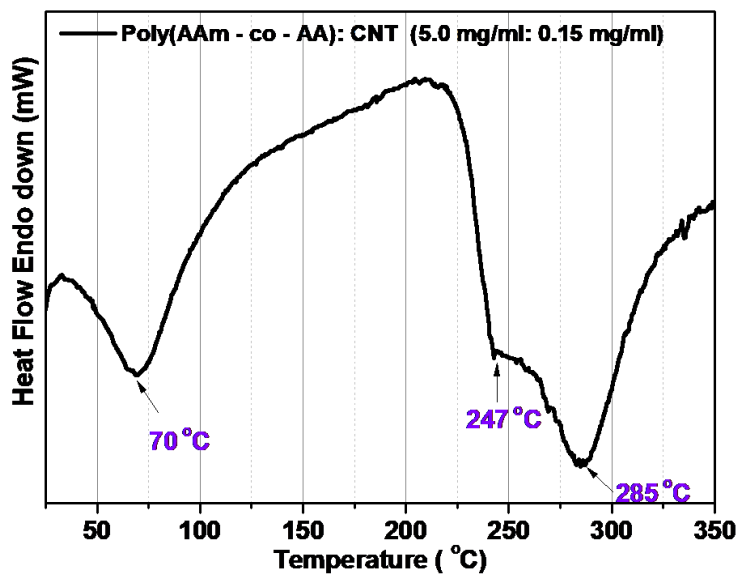


Fig 4.2.b: DSC thermogram of Poly(AAm-co-AA)/CNT(5.0mg/ml:0.15mg/ml)

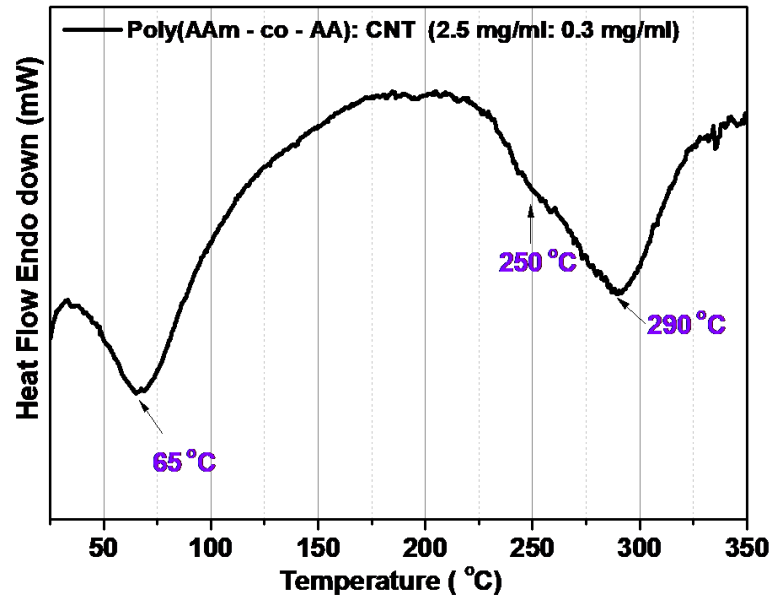


Fig 4.2.c: DSC thermogram of Poly(AAm-co-AA)/CNT(2.5mg/ml:0.3mg/ml)

Table 4.1:DSC results

Sample	Tg (°C)	Tm (°C)	Depth of Tm peak
Poly(AAm-co-AA) film	55	290	Not deep
Poly(AAm-co-AA)/MWNT-COOH (5/0.3)mg/ml	70	282	More than the polymer
Poly(AAm-co-AA)/MWNT-COOH (5/0.15)mg/ml	70	285	More than the polymer
Poly(AAm-co-AA)/MWNT-COOH (2.5/0.3)mg/ml	65	290	More than the polymer

4.2.2 Mechanical Properties of Poly(AAm-co-AA)with CNT-COOH

Figures (4.3.a, b and c) shows the stress-strain curve of Poly(AAm-co-AA), Poly(AAm-co-AA)/CNT-COOH(5.0:0.15)mg/ml. Poly(AAm-co-AA)/CNT-COOH (5.0:0.3)mg/ml respectively. The elongation of Polymer film was around 98%, comparing the young's modulus (Y) for neat polymer and polymer loaded CNT-COOH at different concentrations.

The following results were obtained as follow: the young's modulus for the Poly(AAm-co-AA) is 105%, for Poly(AAm-co-AA)/CNT-COOH (5.0:0.3)mg/ml is 400%, and for Poly(AAm-co-AA)/CNT-COOH (5.0:0.15)mg/ml is 197%, the addition of CNT-COOH plays an important role in the improvement of mechanical properties of hydrogels. Our results show enhancement mechanical properties and it is increased from a good dispersion of CNT on the Polymer matrix, and a strong hydrogen bonding between Poly(AAm-co-AA) and CNT. The increasing of CNT concentration in the matrix of polymer leads to an increase in the (Y) and so the mechanical properties of the nanocomposite. The plastic strain region was noticed that disappeared in the nanocomposite. This is because the nanocomposite behavior was close to the fiber materials' mechanical behavior. These results agree with a search was made in 2004 about PS and MWNT[40]. The researchers got improvement in young's modulus results for PS with 1.0 weight percent of MWNT [40]. The above results also go with 0.3Wt % MWNT nanocomposite of with polypropylene (PP). The tensile strength(TS) and elastic modulus(EM) of the nanocomposite hydrogel increased by 18,4%,and45%, respectively with 0.3% Wt. MWNT loading[35]. The PLA/CNTs/CIN,the TS(MPa), EM(MPa), Elongation($\epsilon\%$) improved by 22.9%,1343%,and 11.87%,respectively with MWNT-COOH[50].

Mechanical Test

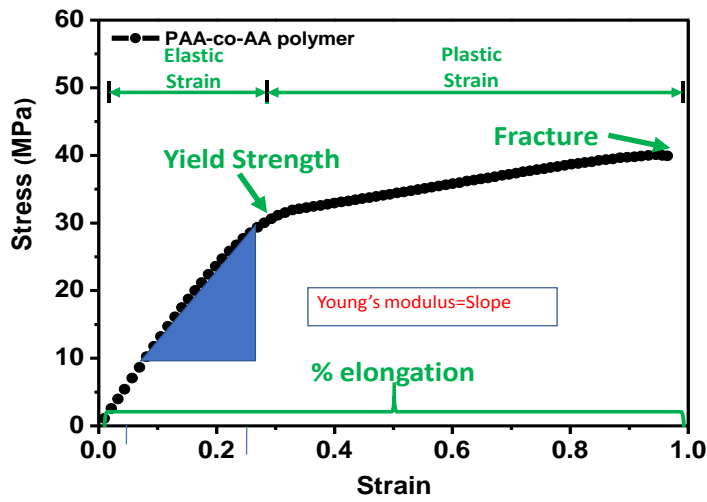


Figure 4.3.a The Stress-Strain of Poly(AAm-co-AA)

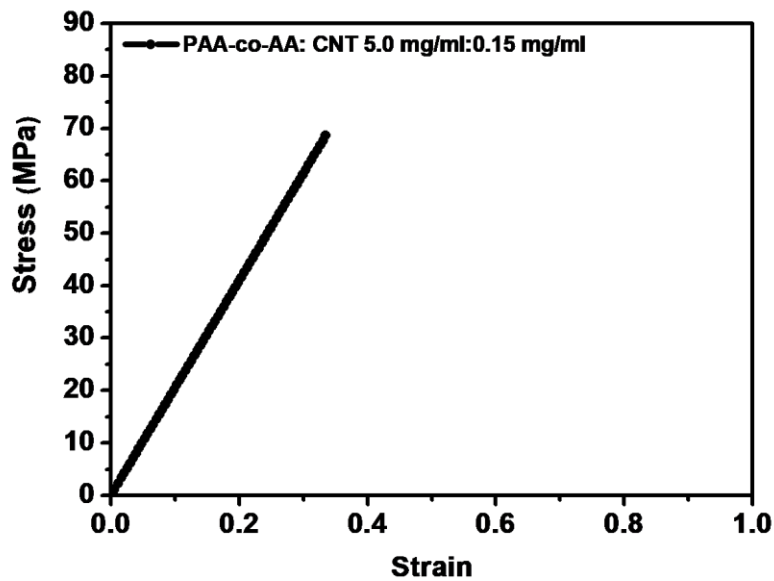


Figure 4.3.b The Stress-Strain curve of Poly(AAm-co-AA)/CNT(5.0:0.15)mg/ml

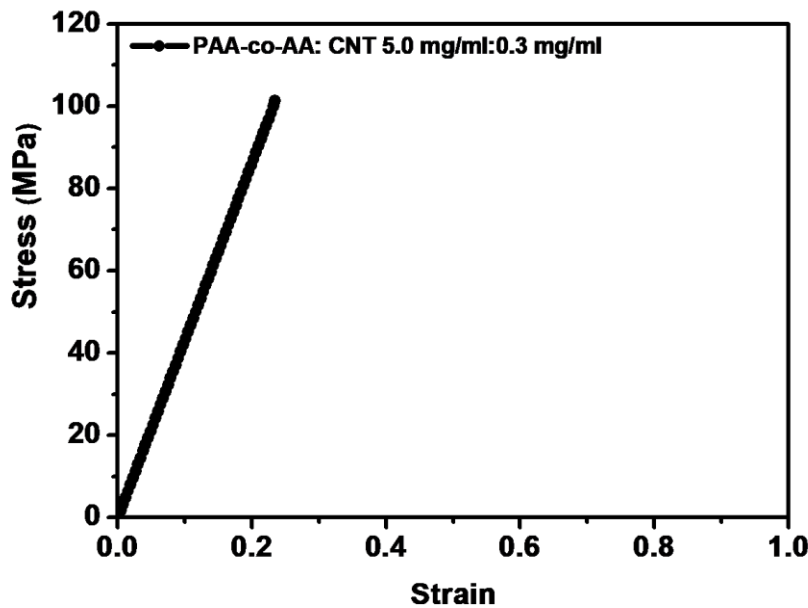


Figure 4.3.c The Stress-Strain of Poly(AAm-co-AA)/CNT(5.0:0.3)mg/ml

4.2.3 Swelling ratio of Polymer Poly(AAm-co-AA)/CNT-COOH

As shown in table 4.2.a, the swelling ratio of Poly(AAm-co-AA) at different concentrations were estimated. The swelling ratio for a polymer with the highest concentration shows the lowest swelling ratio. That's because the strength and the water absorption ability of the hydrogel are low when the amount of cross-linking is high, so the network density increases which leads to lowering the water absorption ability of the hydrogel. From the other hand, the lower concentration of polymer has more porous than that of a higher concentration, so there is more volume between the polymer network for water to go through. In phosphate buffer, the degree of the ionization is enhanced, and electrostatic repulsions among the $-COO^-$ groups are created. This increased repulsive force would push the chain segments apart and attract more water into the hydrogels, and the values of SR increased with an increase in CNTs-COOH concentrations in shown in Table (4.2.b). The reason is that the introduction of the suitable CNTs-COOH loading can effectively improve pH sensitivity and SRs. The higher the CNT-COOH content 0.03% CNT-COOH in the nanocomposite, the higher the swelling ratio obtained more than the 0.015% CNT-COOH.

They indicated in a study published in 2020 that all hydrogels had larger swelling ratios in buffer solutions with higher pH values than in buffer solutions with lower pH values. In other words, as the pH rises, the swelling capacity rises as well. The presence of hydrogen bonding in Poly(AM-co-SMA) networks in an acid media could explain this phenomena. The hydrogen bond complex would prevent network chains from moving or relaxing, resulting in the formation of a compact hydrogel network and a reduced swelling ratio at pH =7 compared to pH =1.4 for P. (AM -co-SMA). [9].

Table4.2 a: Swelling ratio results of Poly(AAm-co-AA)

# of sample	% of P(AAm-co-AA)	% of swelling ratio (SR)
S1	5%	0.21%
S2	2.5%	0.3%
S3	1.25%	0.91%
S4	0.9%	1.67%

Table 4.2 b: Swelling ratio results of P(AA-co-AA)/CNT-COOH

# of sample	%Poly(AA-co-AA)	%CNT-COOH	%Swelling ratio
1	5%	0.03%	0.12%
2	2.5%	0.03%	0.19%
3	1.25%	0.03%	0.75%
4	0.9%	0.03%	1.23%
5	5%	0.015%	0.10%
6	2.5%	0.015%	0.17%
7	1.25%	0.015%	0.66%
8	0.9%	0.015%	1.15%

4.2.4 Quality Assurance (IR of Functionalized CNT-COOH and Poly (Acryl amide- co- acrylic acid))

4.2.4.1 FT-IR of Pure Poly(AAm-co-AA) and Pure CNT-COOH

In order to obtain information about the structures of different hydrogels, including the pure Polymer and nanohybrid hydrogels such as Poly (AAm-co-AA)/CNT-COOH, we carried out the examination of the FTIR spectra. According to the FT-IR spectrum of Poly(AAm-co-AA) as shown in Fig(4.4.a), the functional groups were observed as the following: NH₂, CH₂, C=O, C–N can be assigned at the bands of 3337 cm⁻¹, 3190 cm⁻¹, 1646 cm⁻¹, 1428 cm⁻¹ respectively. At 1118 cm⁻¹ is another peak related to the amide group. The peak appearing at 1322cm⁻¹ is the characteristics (C–O) bending peak of –COOH, the FT-IR spectrum of CNT-COOH is shown in Fig(4.4.b), the oxygen functional group were observed as the following: C=O and C-O can be assigned at the bands of 1635 cm⁻¹, 1068cm⁻¹respectively. The hydroxyl group (O-H) can be noticed at 3300cm⁻¹. C=C group appeared at 1404 cm⁻¹.

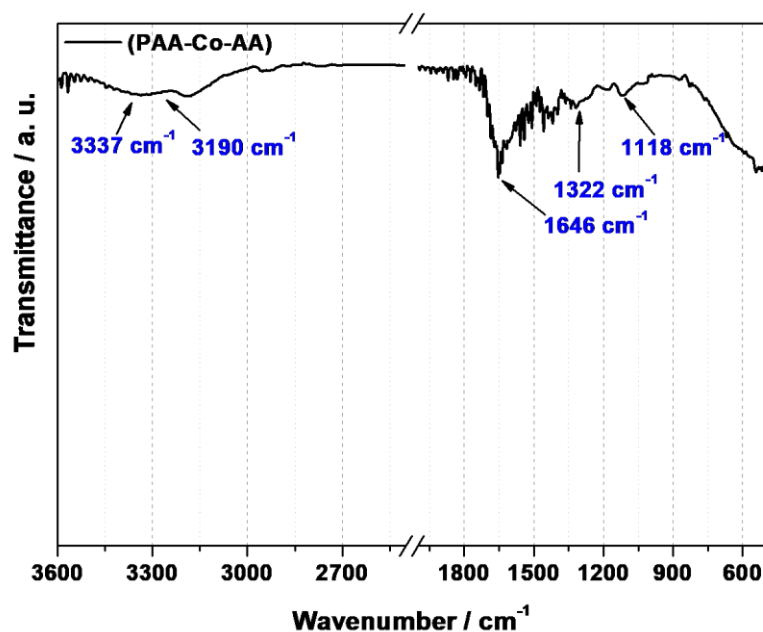


Fig 4.4.a: FTIR spectrum of Poly(AAm-co-AA).

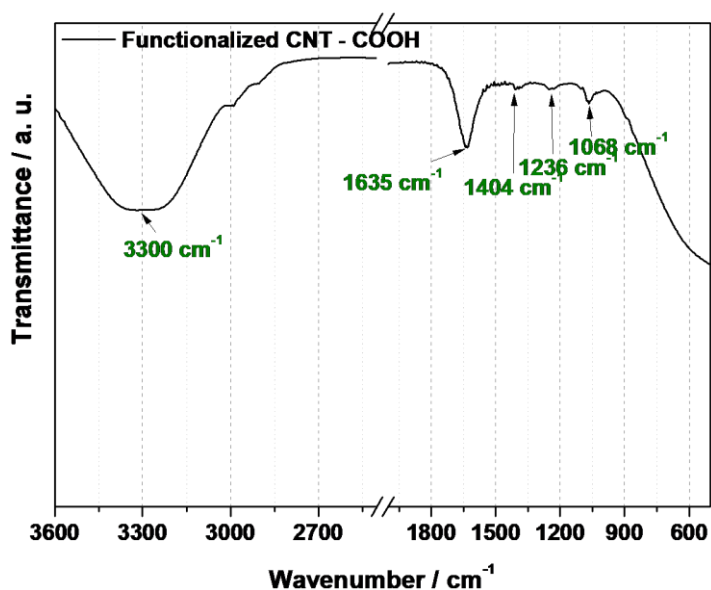


Fig 4.4.b: The FTIR spectrum of Functionalized CNT-COOH.

4.2.4.2 FT-IR of Poly (AAm-co-AA)/CNT-COOH

In order to obtain information about the structures of different nanohybrid hydrogels such as Poly (AAm-co-AA)/CNT-COOH, we carried out the examination of the FTIR spectra.

The shift of CH₂, C=O, CN, and COOH groups can be assigned to the interaction that occurred between Poly(AAm-co-AA) and MWNT-COOH. At all concentrations of Poly(AA-co-AA) the shifts are clear whether to lower frequency happened a change in the interatomic distance along with the bond (bending vibration), and in the higher frequency a change in the angle of peaks (stretching vibration), as shown in Fig (4.5 a, and b).

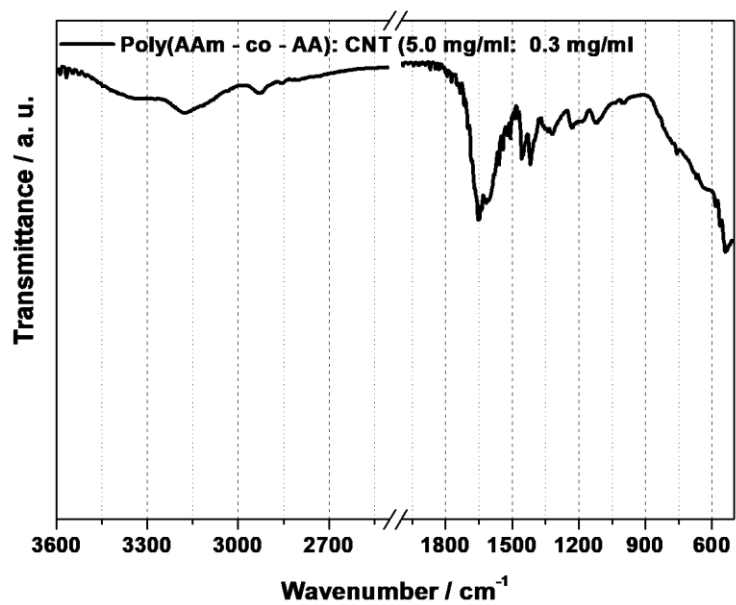


Fig4.5. a The FT-IR spectrum of Poly(AAm-o-AA)/CNT(5.0:0.3)mg/ml

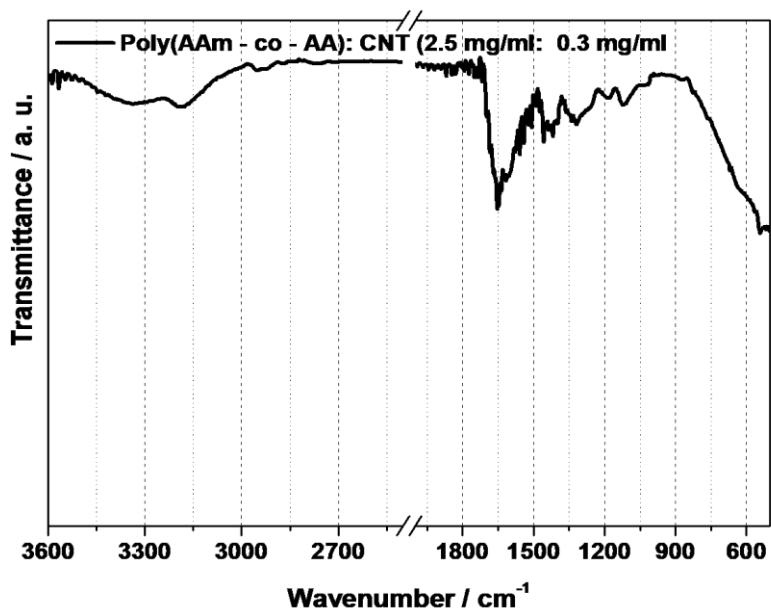


Fig 4.5.b The FT-IR spectrum of Poly(AAm-o-AA)/CNT(2.5:0.3)mg/ml

Table(4.3):FT-IR results for each of Poly (AAm-co-AA) film,CNT-COOH,Poly(AAm-co-AA)/CNT-COOH nanocomposite.

Functional groupe name	Wavelength of Poly(AAm-co-AA) (cm ⁻¹)	Wavelength of CNT-COOH(cm ⁻¹)	Wavelength of Poly(AA-co-AA) with CNT nanocomposite (cm ⁻¹)	Shifting
O-H	-	3300	-	-
NH ₂	3337	-	3323	14 –Right
CH ₂	2850	-	2850	-
C=O	1646	1635	1650	4-Left
C-N	1428	-	1416	12-Right
C=C	-	-	1612	-
COOH	1322	1236	1237	85-Left

4.2.5 Thickness test of P(AAm-co-AA), P(AAm-co-AA)/CNT-COOH nanocomposite.

The thickness of Poly (AAm-co-AA), films, and Poly(AAm-co-AA)/CNT-COOH nanocomposite was measured by using caliber and calculations: Each film was weight separately in order to get the mass.

The following equations were used for calculations.

$$V=L \times W \times H$$

V: volume ,L: length ,W: width H: Hight

$$D=M/V$$

D: Density ,M: Mass, V: Volume

The thickness of Polymer and Poly(AAm-co-AA)/CNT-COOH was maintained between 0.043 to 0.33 mm,that means as the concentration increased the thickness increased.As show Table 4.4.

Table 4.4: Thickness results for polymer alone by calculation and caliber and Poly(AAm-co-AA)/CNT-COOH by caliber

Poly(AAm-co-AA)%	CNT-COOH%	Thickne ss by caliber (mm)	Thickne ss by calculations (mm)	Total average
5%	-	0.325	0.295	0.1408
2.5%	-	0.133	0.095	
1.25%	-	0.060	0.055	
0.9%	-	0.045	0.04	
5%	0.03%	0.334	-	0.1505
2.5%	0.03%	0.151	-	
1.25%	0.03%	0.067	-	
0.9%	0.03%	0.050	-	
5%	0.015%	0.333	-	0.1453
2.5%	0.015%	0.142	-	
1.25%	0.015%	0.063	-	
0.9%	0.015%	0.043	-	

5. Conclusion and future work

The preliminary assessments have shown that a Poly(AAm-co-AA)/CNT-COOH nanocomposite films were prepared by a simple casting method.

as the interaction between the polymer and the carbon nanotube leads to improving the thermal properties, so it leads to an increase in T_g , crystallization temperature, and a decrease in melting and degradation.

The hydrogels presented good equilibrium water absorbency, and barrier properties of CNT-COOH were interpreted by increasing in swelling as the concentration of CNT-COOH increased in solution (PH=7), and high compression mechanical properties, satisfactory pH behavior.

Fourier transform infrared (FTIR) has confirmed that Poly(AAm-co-AA) networks covered the CNT-COOH closely due to the strong interaction, and different microporous or sub microporous structures have been formed.

In the future, it will be applied to pharmaceutical packaging such as a capsules shell in drugs that included hydrophilic and hydrophobic ingredients.

REFERENCES

1. Nesrinne, S. and A. Djamel, Synthesis, characterization and rheological behavior of pH sensitive poly (acrylamide-co-acrylic acid) hydrogels. *Arabian Journal of Chemistry*, 2017. **10**(4): p. 539-547.
2. Craciun, G., et al., Synthesis and characterization of poly (acrylamide-co-acrylic acid) flocculant obtained by electron beam irradiation. *Materials Research*, 2015. **18**: p. 984-993.
3. Mahon, R., et al., Swelling performance of sodium polyacrylate and poly (acrylamide-co-acrylic acid) potassium salt. *SN applied sciences*, 2020. **2**(1): p. 1-15.
4. Dresselhaus, M.S., et al., Carbon nanotubes, in *The physics of fullerene-based and fullerene-related materials*. 2000, Springer. p. 331-379.
5. Mahar, B., et al., Development of carbon nanotube-based sensors—a review. *IEEE Sensors Journal*, 2007. **7**(2): p. 266-284.
6. Aram, E. and S. Mehdipour-Ataei, Carbon-based nanostructured composites for tissue engineering and drug delivery. *International Journal of Polymeric Materials and Polymeric Biomaterials*, 2021. **70**(16): p. 1167-1188.
7. Asadi, N., et al., Fabrication and in vitro evaluation of Nanocomposite hydrogel scaffolds based on gelatin/PCL-PEG-PCL for cartilage tissue engineering. *ACS Omega*, 2019. **4**(1): p. 449-457.
8. Patel, D.K., et al., Carbon nanotubes-based nanomaterials and their agricultural and biotechnological applications. *Materials*, 2020. **13**(7): p. 1679.
9. Liu, Z., Z. Yang, and Y. Luo, Swelling, pH sensitivity, and mechanical properties of poly (acrylamide- co- sodium methacrylate) nanocomposite hydrogels impregnated with carboxyl- functionalized carbon nanotubes. *Polymer composites*, 2012. **33**(5): p. 665-674.
10. Sadegh, H., et al., Synthesis of MWCNT-COOH-Cysteamine composite and its application for dye removal. *Journal of Molecular Liquids*, 2016. **215**: p. 221-228.
11. Hahm, M.G., et al., A review: controlled synthesis of vertically aligned carbon nanotubes. *Carbon letters*, 2011. **12**(4): p. 185-193.
12. Dresselhaus, G., M.S. Dresselhaus, and R. Saito, *Physical properties of carbon nanotubes*. 1998: World scientific.
13. Ebbesen, T., et al., Electrical conductivity of individual carbon nanotubes. *Nature*, 1996. **382**(6586): p. 54-56.

14. Ibrahim, K.S., Carbon nanotubes-properties and applications: a review. Carbon letters, 2013. **14**(3): p. 131-144.
15. Ajayan, P., et al., Aligned carbon nanotube arrays formed by cutting a polymer resin—nanotube composite. science, 1994. **265**(5176): p. 1212-1214.
16. Ruoff, R.S. and D.C. Lorents, Mechanical and thermal properties of carbon nanotubes. carbon, 1995. **33**(7): p. 925-930.
17. Hernandez, E., et al., Elastic properties of C and B x C y N z composite nanotubes. Physical Review Letters, 1998. **80**(20): p. 4502.
18. Khandoker, N., et al., Tensile strength of spinnable multiwall carbon nanotubes. Procedia Engineering, 2011. **10**: p. 2572-2578.
19. Moreno-Castilla, C., et al., Effects of non-oxidant and oxidant acid treatments on the surface properties of an activated carbon with very low ash content. Carbon, 1998. **36**(1-2): p. 145-151.
20. Cao, Y., Applications of cellulose nanomaterials in pharmaceutical science and pharmacology. Express Polymer Letters, 2018. **12**(9).
21. Popov, V.N., Carbon nanotubes: properties and application. Materials Science and Engineering: R: Reports, 2004. **43**(3): p. 61-102.
22. Yu, C., et al., Thermal conductance and thermopower of an individual single-wall carbon nanotube. Nano letters, 2005. **5**(9): p. 1842-1846.
23. Perkins, B. L., et al., Carbon nanostructures in bone tissue engineering. The open orthopaedics journal, 2016. **10**, 877
24. Pei, B., et al. Applications of carbon nanotubes in bone tissue regeneration and engineering: superiority, concerns, current advancements, and prospects. Nanomaterials, 2019 **9**(10), 1501
25. Wu, D., et al., DNA nanostructure-based drug delivery nanosystems in cancer therapy. International Journal of Pharmaceutics, 2017. **533**(1): p. 169-178.
26. Yadav, A.R. and S.K. Mohite, Carbon nanotubes as an effective solution for cancer therapy. Research Journal of Pharmaceutical Dosage Forms and Technology, 2020. **12**(4): p. 301-307.
27. Kausar, A., Nanocarbon in polymeric nanocomposite hydrogel—design and multi-functional tendencies. Polymer-Plastics Technology and Materials, 2020. **59**(14): p. 1505-1521.

28. Bharadwaz, A. and A.C. Jayasuriya, Recent trends in the application of widely used natural and synthetic polymer nanocomposites in bone tissue regeneration. *Materials Science and Engineering: C*, 2020. **110**: p. 110698.
29. Chowdhury, R., A review on the application of nanotechnology in pharmaceutical science. 2015, East West University.
30. Jadhav, S.P., et al., Nanotechnology in Pharmaceutical Science: A Concise Review.
31. Cao, Y., Applications of cellulose nanomaterials in pharmaceutical science and pharmacology. *Express Polymer Letters*, 2018. **12**(9).
32. Muhammad, G., et al., Glucuronoxylan-mediated silver nanoparticles: green synthesis, antimicrobial and wound healing applications. *RSC advances*, 2017. **7**(68): p. 42900-42908.
33. Vellayappan, M., S. Jaganathan, and A. Manikandan, Nanomaterials as a game changer in the management and treatment of diabetic foot ulcers. *RSC advances*, 2016. **6**(115): p. 114859-114878.
34. Sharma, D. and C.M. Hussain, Smart nanomaterials in pharmaceutical analysis. *Arabian Journal of Chemistry*, 2020. **13**(1): p. 3319-3343.
35. Beg, S., et al., Emergence in the functionalized carbon nanotubes as smart nanocarriers for drug delivery applications, in *Fullerens, Graphenes and Nanotubes*. 2018, Elsevier. p. 105-133.
36. Jildeh, N.B. and M. Matouq, Nanotechnology in packing materials for food and drug stuff opportunities. *Journal of Environmental Chemical Engineering*, 2020. **8**(5): p. 104338.
37. Chelliah, R., et al., Development of Nanosensors Based Intelligent Packaging Systems: Food Quality and Medicine. *Nanomaterials*, 2021. **11**(6): p. 1515.
38. do Amaral Montanheiro, T.L., et al., Effect of MWCNT functionalization on thermal and electrical properties of PHBV/MWCNT nanocomposites. *Journal of Materials Research*, 2015. **30**(1): p. 55-65.
39. Yetgin, S.H., Effect of multi walled carbon nanotube on mechanical, thermal and rheological properties of polypropylene. *Journal of Materials Research and Technology*, 2019. **8**(5): p. 4725-4735.
40. Harris, P., F. Carbon nanotube composites. *International Materials Reviews*, 2004. **49**(1): p. 31-43.
41. Xia, H. and M. Song, Preparation and characterization of polyurethane-carbon nanotube composites. *Soft Matter*, 2005. **1**(5): p. 386-394.

42. Dabees, S., et al., Wear performance and mechanical properties of MWCNT/HDPE nanocomposites for gearing applications. *Journal of Materials Research and Technology*, 2021. **12**: p. 2476-2488.
43. Bardajee, G.R., et al., Synthesis of magnetic multi walled carbon nanotubes hydrogel nanocomposite based on poly (acrylic acid) grafted onto salep and its application in the drug delivery of tetracycline hydrochloride. *Colloids and Surfaces A: Physicochemical and Engineering Aspects*, 2021. **616**: p. 126350.
44. Mohammadinezhad, A., et al., Synthesis of poly (acrylamide-co-itaconic acid)/MWCNTs superabsorbent hydrogel nanocomposite by ultrasound-assisted technique: swelling behavior and Pb (II) adsorption capacity. *Ultrasonics Sonochemistry*, 2018. **49**: p. 1-12.
45. Liu, Z., Z. Yang, and Y. Luo, Swelling, pH sensitivity, and mechanical properties of poly (acrylamide- co- sodium methacrylate) nanocomposite hydrogels impregnated with carboxyl- functionalized carbon nanotubes. *Polymer composites*, 2012. **33**(5): p. 665-674.
46. Masjoudi, M., et al., Pharmaceuticals removal by immobilized laccase on polyvinylidene fluoride nanocomposite with multi-walled carbon nanotubes. *Chemosphere*, 2021. **263**: p. 128043.
47. Kim, H.J., et al., Mechanical and electrical properties of carbon nanotube fibers from impregnation with poly (vinyl alcohol)/poly (acrylic acid) and subsequent thermal condensation. *Polymer Composites*, 2018. **39**(3): p. 971-977.
48. Salem, K.S., et al., The effect of multiwall carbon nanotube additions on the thermo-mechanical, electrical, and morphological properties of gelatin–polyvinyl alcohol blend nanocomposite. *Journal of Composite Materials*, 2015. **49**(11): p. 1379-1391.
49. Wu, C.-S. and H.-T. Liao, Study on the preparation and characterization of biodegradable polylactide/multi-walled carbon nanotubes nanocomposites. *Polymer*, 2007. **48**(15): p. 4449-4458.
50. Cui, R., et al., Antimicrobial film based on polylactic acid and carbon nanotube for controlled cinnamaldehyde release. *Journal of Materials Research and Technology*, 2020. **9**(5): p. 10130-10138.

تحضير ووصف مركب الكاربون نانوتيوب مضاف إليه مجموعة الكربوكسل الوظيفية مع حمض البوليأكريل أميد المشترك لتطبيقات تغليف المستحضر الصيدلانية

إعداد الطالبة: تغريد أكرم محمد قاطقة

المشرف الرئيسي: الدكتور سامي مخرزة – جامعة الخليل

المشرف الثاني: الدكتور وديع سلطان

الملخص:

لقد استخدمنا الكاربون نانوتيوب متعدد الجدران مضاف إليه مجموعة الكربوكسل بواسطة عملية الكربوكسل ليتم دمجها مع بوليمر حمض بولي أكريل أميد كو أكريليك المشترك من أجل دراسة الخصائص الحرارية والميكانيكية وكذلك اختبار التورم. تم استخدام تراكيز مختلفة من بوليمر حمض بولي أكريل أميد كو أكريليك (5, 1.25, 2.5, 0.9) % مع تراكيز مختلفة من الكاربون نانوتيوب متعدد الجدران (0.03 و 0.015) % لتحضير مركب النانو حمض بولي أكريل أميد كو أكريليك/ كاربون نانوتيوب باستخدام طريقة الصب البسيطة. تم دراسة الخواص الحرارية باستخدام مسعر المسح التبايني وأظهرت النتائج أن الخواص الحرارية تحسنت من خلال دمج الكاربون نانوتيوب مع بوليمر حمض بولي أكريل أميد كو أكريليك المشترك. زادت درجة حرارة التزجج من 55 لبوليمر حمض بولي أكريل أميد كو أكريليك النقي إلى 70 درجة مئوية عند إضافة 0.03، 0.015% من الكاربون نانوتيوب، حيث تم زيادة البلورية إلى حد معين. وهذا يدل على أن جزء من البوليمر تحول من الشكل اللابلوري إلى الشكل البلوري مما يؤدي إلى التقليل في المسافات بين سلاسل البوليمر، وهذا دليل على زيادة صلابته. قوة الشد في بوليمر حمض بولي أكريل أميد كو أكريليك زادت بزيادة نسبة جزيئات الكاربون النانوية إلى 400% عندما كان تركيز الكاربون نانوتيوب 0.03%. زادت نسبة تورم البوليمر المحضر بتركيزات مختلفة بإضافة الجسيمات نانوية بسبب زيادة الترابط الهيدروجيني الحاصل من مجموعة الكربوكسل. تؤكد نتائج أطيف تحويل فورييه الطيفي بالأشعة تحت الحمراء لتحليل المركبات النانوية أن بوليمر (حمض بولي أكريل أميد كو أكريليك) مع الكاربون نانوتيوب متعدد الجدران المضاف إليه مجموعة الكربوكسل على حدوث ترابط قوي بين البوليمر والجسيمات النانوية في عدة مجموعات وظيفية. باختصار، أدى دمج جسيمات الكاربون النانوية في مصفوفة البوليمر وهو حمض بولي أكريل أميد كو أكريليك إلى تحسين الخواص الحرارية والميكانيكية للبوليمر، بسبب التفاعل القوي بين جزيئات البوليمر والمركب النانو.

•
•